Poster Setup and Presentation Times

Poster Presentation Times

(Please plan to attend your posters during the following times)

Sunday, June 21 (Welcome Reception)..... 6:00 PM–6:30 PM
Monday, June 22..... 9:45 AM–10:15 AM and 3:00 PM–3:30 PM
Tuesday, June 23 .....10:00 AM–10:30 AM
Wednesday, June 24.....10:00 AM–10:30 AM

Poster Setup

Sunday, June 21 ..... 12:00 Noon–5:00 PM

Poster Teardown

Wednesday, June 24.....1:00 PM–2:00 PM

If your poster is not removed before 2:00 PM, it will be removed and placed outside the Exhibit Hall.

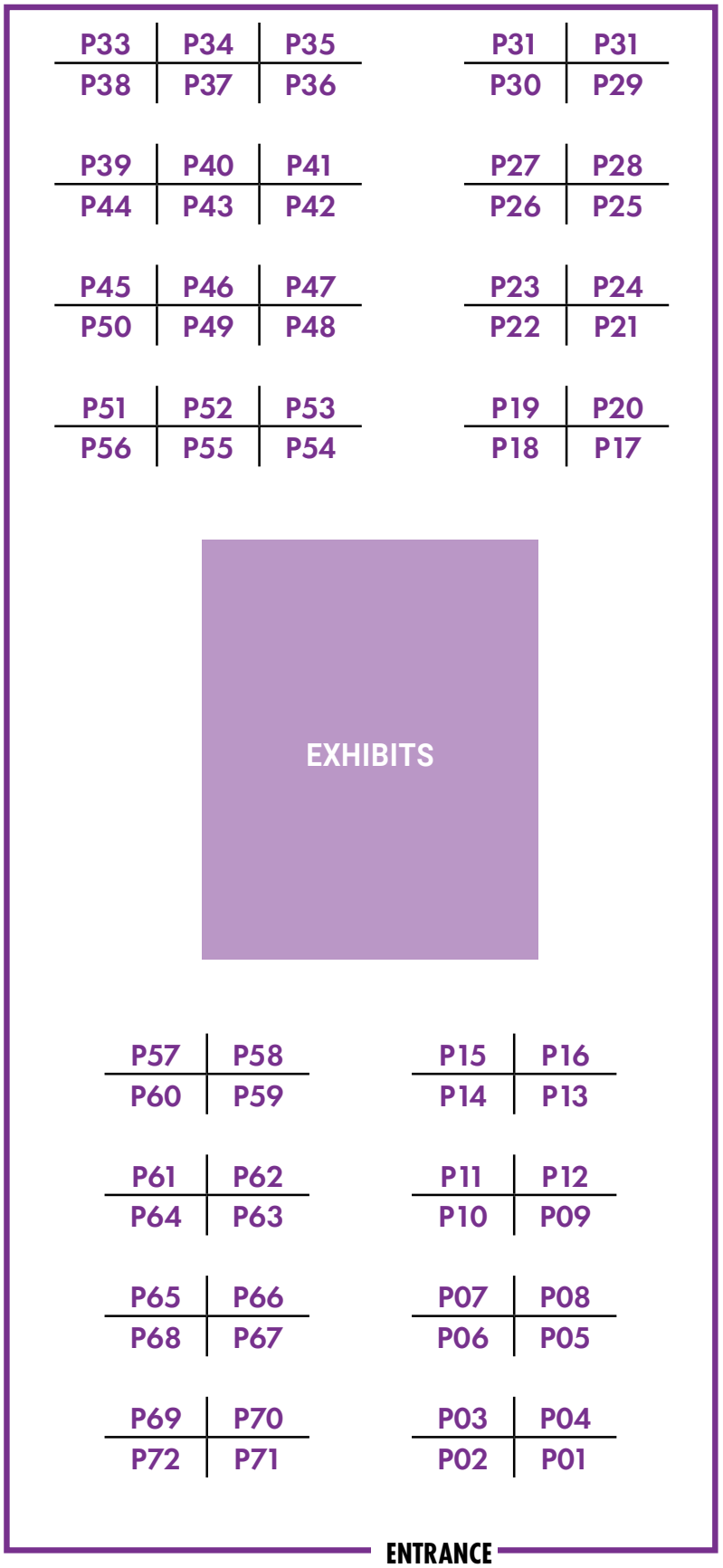

Poster Presentation Index

Poster Categories

P01 Utility of Immunohistochemical Characterization of Prechronic Lung Lesions as Early Markers of Chemical-Induced Carcinogenesis in Rodent Toxicology Studies
Mallikarjun Bidarimath, Mark F. Cesta, Robert C. Sills, Sonika Patial

P02 Chronic Liver Toxicity Promotes Liver Fibrosis by Hepatocyte Dedifferentiation Into Myofibroblast-Like Cells Through the TGF-β1-Oct4 Axis
Manisha Yadav, Shobhit Verma, Smriti Verma, Madhav Nilakanth Mugale

P03 Hsd17b7 Is Required for Proper Mammalian CNS Development
Bayla Bessemer, Rolf Stottmann

P04 Sectional and Transmural Variation in Ultrastructural Morphology of the Left Ventricle in Canine Primary Dilated Cardiomyopathy
Mark D. Bilger, Lisa Freeman

P05 MRP4 Modulates Hepatic Response to Phenobarbital by Regulating Proliferative and Metabolic Pathways
Ankit P. Laddha, Hangyu Wu, José E. Manautou

P06 Loss of Brain Resilience with microRNA-29 Reduction in the Context of Alzheimer's Disease
Jonathan Nagel, Nazanin Kiapour, Keeley Spiess, Sheryl Moy, Mohanish Deshmukh

P07 Can You Identify Hepatic Sinusoidal Lining Cells On HE Sections?
Hinata Niimi, Mitsuru Kuwamura, Takeshi Izawa

P08 Autopsy-Based Evidence of Early Hepatocellular Injury in Fatal Glyphosate Poisoning in a 16-Year-Old Girl
Mrinal Patnaik, Poonam Patnaik

P09 Microscopic Nomenclature Used in Evaluation of Nonclinical Wound Healing Studies: Highlighting Gaps in Current INHAND Terminology
Elise M. Peauroi, Sarah Davis, Lyn M. Wancket

P10 An Indian Traditional Medicine – Vasant Kusumakar Rasa Ameliorates Renal Damage in Diabetic Rats
Alok D. Singh, Mukesh B. Chawda, Yogesh A. Kulkarni

P11 Identification of Disease-Associated Polyomaviruses from Cynomolgus Macaques Undergoing Stem Cell Transplantation
Helena Vogel, Tristan T. Neal, Helen L. Wu, Paul Kievit, Jonah B. Sacha, Gabriel J. Starrett

P12 Modeling Th2-Driven Pathogenesis of Atopic Dermatitis Using Canine Primary Epidermal Organoids
Bo Chen, Ron Slocombe, Yuanting Zheng, Mirjana Bogeski, Oluwadamilola Samuel Omotainsea, Smitha Rose Georgy

P13 From Constraints to Capability: Developing a User-Friendly Deep Learning Framework in a Cost-Constrained Research Environment
Brian R. LaMendola, Rachael M. Wolters, Altair E. Fazio, Nathan P. Crilly

P14 A Two-Phase Validation Framework Informed by an *In Vitro* Cardiotoxicity Screening Case Study
Yigunag Zhu, Kathleen Gabrielson, Mark Kohr, Vasiliki Machairaki, Lena Smirnova, Paul A. Locke

P15 Spatiotemporal Analyses of Early Hepatocarcinogenesis Reveal Liver-Resident ILC1s as a Major Player in Early Immune Surveillance
Patrick Huang, Rajiv Trehan, Benjamin Ruf, Chi Ma, Dana Soika, Lorenz Kocheise, Gabriel Bacil Prata, Tim Greten, Firouzeh Korangy

P16 A Novel TGFβ Pathway Reporter Mouse Reveals Stage-Specific Suppression of Mitochondrial Metabolism in Mammary Tumorigenesis
Zachary Millman, Lalage Wakefield, Yu-an Yang

P17 Analyzing the Genetic Basis and Transcriptional Features of Sarcomas in Irradiated Rhesus Macaques
Courtney S. Moore, Karl Dykema, Nury Steuerwald, Mark Cline

P18 Microplastic-Induced Cellular Toxicity: Effects on Connexin 43 and Connexin 26 Expression in Canine Mammary Cell Lines
Guilherme da Silva Rogerio, Ivone Izabel Mackowiack da Fonseca, Maria Lúcia Zaidan Dagli

P19 Antileukemic Potential of Hydroalcoholic Extract of *Fagonia cretica* L. in Benzene-Induced Leukemia in Rats
Adeeba Zaidi, Nasreen Jahan

P20 Severe Ocular Necrotizing Vasculopathy Following Suprachoroidal Delivery of a Polymeric Formulation in a Rhesus Macaque
Akhil A. Vinithakumar, Katharina M. Gregor, Mirella Rivera-Velazquez, Sarah E. Cook, Marie-Josee Marie-France Lemoy, Rebecca L. Sammak, Glenn Yiu, Katherine J. Olstad

P21 Treatment with Small-Molecule Biofilm Inhibitors in a Novel Murine Model of Chronic Typhoid Fever
Allysa L. Cole, John S. Gunn

P22 *Staphylococcus aureus* Superantigens Suppress Sebaceous Gland Lipids to Promote Skin Colonization
Laine E. Feller, Zhiyang Li, Diane Hong, Toan Bui, Sabrina Kline, Meng-Jen Wu, Jing Zhang, Yu Wang, Shardulendra P. Sherchand, M. Javad Aman, Stephen W. Tuffs, Heidi H. Kong, Sima Rozati, Nathan K. Archer

P23 Historical Microscopic Control Data of the Central and Peripheral Nervous System in Beagles
Samantha Hicks-Peña, Charlotte Hollinger, Molly Liepnieks, Sarah Coe

P24 Poster Withdrawn

P25 Hepatotoxicity Associated with Portosystemic Shunts in C57BL/6J Mice Fed a High Fat Diet with Butylated Hydroxyanisole
Claire Kazen-Thompson, Rani S. Sellers, Summer Truong, Tigist Tamir

P26 Novel Double *abcb4/abcg2a* Knockout Zebrafish Model for Studying ABC Transporter–Mediated Drug Efflux and Toxicity
Chaunte Lewis, Joanna Thomas, Blake Carrington, Kevin Bishop, Robert Robey

P27 Recovery Mechanism of Drug-Induced Vacuolar Lesions of the Adrenal Cortex After Drug Withdrawal
Ryo D. Obara, Yuki Kato, Yoshiji Asaoka, Yukie Murata, Hiroyuki Oka, Takeshi Izawa, Mitsuru Kuwamura

P28 Comparative Evaluation of Historical Control Hematology, Coagulation, and Clinical Chemistry Test Results between Sprague-Dawley and Wistar-Han Rats
Vasilis C. Pliasas, Charles E. Wiedmeyer

P29 Immunohistochemical Delineation of Macrophage Functional States for Disease Characterization
Dayananda Siddappa, Ingeborg M. Langohr, Catherine King, Tatyana Taksir, Cynthia Shapiro, Colleen Maloney, Agnes Cheong, Timothy Hammond, Caroline Morel, Dinesh S. Bangari

P30 Azoxymethane-Treated Pirc Rats as an Accelerated Model of Colorectal Cancer
Allison C. Boone, Ricardo Cortes, Xuying Zhang, Krishna Latha Kanchi, Willie Cunningham, Peter Pediaditakis, Thai-Vu Ton, Arun Pandiri

P31 Brain Pathology in Irradiated Nonhuman Primates: Vascular Injury is Radiation Dose Dependent
Clemer Abad, John Olson, George Schaaf, J. Mark Cline

P32 Comparative Pathology of a Macaque Model of Bardet-Biedl Syndrome due to BBS7 Mutation
Nathan P. Crilly, Brian Lamendola, Anne Lewis, Kathy Grant

P33 Assessment of Orchidometric Testicular Volume as a Tool for Selecting Sexually Mature Male Rhesus Monkeys for Nonclinical Toxicology Studies
Maria C. Cuitino, Takayuki Tsuchiya, Sabu Kuruvilla

P34 INHAND: International Harmonization of Nomenclature and Diagnostic Criteria for Lesions—An Update
Emily Meseck, Ute Bach, Alys Bradley, Mark Cesta, Stacey Fossey, Shimmo Hayashi, Matt Jacobsen, Rupert Kellner, Victoria Laast, Thomas Nolte, Kumiko Ogawa, Susanne Rittinghausen, Junko Sato, John Vahle, Katsuhiko Yoshizawa

P35 Comparison of Background Histologic Findings in Cynomolgus Macaques of Philippine vs. Other Asian Origin
Melissa Graham, Kelly Ashcroft-Hawley, Lars Mecklenburg, Julie Turner, Jim Saul, Victoria Laast, Alok Sharma

P36 Reference Intervals for Clinical Pathology Parameters in Sprague-Dawley Rats in Juvenile Animal Toxicity Studies
Aradhana Gupta, Stavros Zinonos, Lindsay Tomlinson, Taylor Hulten, Stephanie S. Powlin, Nicola Powles Glover, Keith R. Shockley, Alan M. Hoberman, Zhiyong Xie, Stephanie L. Rayhon, Tacey White, Shermaine Mitchell-Ryan, Connie L. Chen

P37 Regional Differences in Tissue Responses After Stent Deployment in Subclavian and Carotid Arteries in Swine Model
Atsushi Isobe, Ryan Callahan

P38 Poster Withdrawn

P39 Dose-Dependent Early Fibrotic Remodeling in a Recurrent LPS-Induced Acute Lung Injury Rat Model: Translational Implications for Human ALI
Predrag Novakovic, Bo In Choi, Alexander-Yap Sia, Joseph Younan, William Lee, Kevin McInally

P40 Background Thymic Epithelial Hyperplasia and Thymoma in rasH2 Transgenic Mice from 26-Week Carcinogenicity Studies
Sasmita Mishra, Vimala Vemireddi, Marcia Pereira Bacare, Molly Boyle, Mark Mense, Alok Sharma

P41 Renal Tubular Injury in Naturally Occurring Arsenic Toxicosis in Cattle with Suspected Waterborne Exposure
Nikhil Sanjay Rao, Jenna Stockler, Rachel Neto

P42 Impact of Duration and Setting of Urine Collection on Urinalysis and Urine Chemistry Parameters in Non-Human Primates
Tiffany N. Scott, Frederic Morel, Gabriella Diamantino, Liza Bau-Gaudreault, Florence Poitout

P43 Phenotypic Characterization of Fra-2 Transgenic Mice as a Model of Scleroderma
Yinglin Gao, Traci Wilgus, Luis Cheng, Bharathi Sundaram, Ted Kaplan, Abigail Gagliardi, Susannah Brydges, Lori Morton, Jon Popke, Prachi Sharma

P44 Toxicological Profile of Therapeutic Radionuclides and Radiopharmaceuticals in Animal Studies: A Scoping Review
Jong Il Shin, Jin Young Baik, Yiseul Choi, Eun Sang Lee, Yong Jin Lee, Kwang Il Kim

P45 Procedure-Related Findings Associated with Subcutaneous Injection in Non-Human Primates Utilized in Preclinical Toxicity Studies
Nick Vetter, Keith Nelson

P46 Application of an Artificial Intelligence Model for Quantitative Evaluation of Rat Bone Marrow Cell Lineages in Toxicology Studies
Mehrdad Ameri, Deon Hildebrand, Peter Clements

P47 Performance of a Single-Class Unsupervised Foundation Model-Based AI Histology Anomaly Detector on Rat Heart from Nonclinical Toxicology Studies
Thomas Forest, Tiffany Jenkins, Roujia Wang, Kyathanahalli Janardhan, Takayuki Tsuchiya, Rajath Soans, Lin Li, Tosha Shah, Raghav Amaravadi, Geetank Raipuria, Nitin Singhal

P48 Enumeration and Laser Capture of Lung Cancer Metastasis in a Mouse Model Using AI Workflows
Raisa Glabman, Amanda Koehne, Jacob Kennedy, Shivani Srivastava

P49 **Automated Quantification of Airway Epithelial Cell Composition in Complex *In Vitro* Models Using Deep Learning–Based Image Analysis**
Van Hovenga, Steven Laing, Christy Chu, Daniel Simmons, Mike Reichelt, Lenitza Nives Lopez

P50 **Optimization of *In Situ* Hybridization (ISH) Staining in Human Tissue Microarrays: Addressing RNA Quality and Background in Challenging Tissues**
Emily M King, Kevin Maisonave, Lydia Andrew-Jones, Amanda Krempley, Magali Guffroy, Stacey Fossey

P51 **Uncharted Territories: Leveraging MALDI-MSI in the Canine Brain as a Novel Translational Neurology Platform**
Sophie R. Nelissen, Rinat Abzalimov, Shu Zhang, Elena A. Demeter

P52 **Teratoma Formation Assay in Immunocompromised Mice to Evaluate Risk of Pluripotent Stem Cell-Derived Cell Therapy Products**
Tyler J. Peat, Sasmita Mishra, Brian E. McIntosh, Mayuri S. Prasad, Susan Lynk, Pamela E. Blackshear

P53 **Agentic Artificial Intelligence System for Preclinical Toxicologic Study Report Drafting via Integrated Data Analysis, Research and Reasoning**
Nasir Rajpoot, Adnan Khan, Mostafa Jahanifar, David Snead

P54 **A Cell-Based Protein Array, the Membrane Proteome Array (MPA), to Assess Off Target Binding Across the Full Human Membrane Proteome**
Jonathan Richards, Diana Norden, Carmen Navia, J. Tabb Sullivan, Benjamin J. Doranz

P55 **Unsupervised Deep Learning-Based Image Analysis Model for Detecting Unlearned Findings in Rat Testis**
Taishi Shimazaki, Yuzo Yasui, Naohito Yamada, Vedang Kshirsagar, Saketh Juturu, Pranab Samanta, Raghav Amaravadi, Toshiyuki Shoda

P56 **Development of a Predictive Model Combining HPV DNA Genotyping and E6/E7 mRNA Testing for the Diagnosis of Cervical Precancerous Lesions**
Jingzheng Ye

P57 **Tafazzin Overexpression with High Dose AAV in Tafazzin Knockdown Mice Leads to Cardiotoxicity**
Elizabeth L. Buza, Nicholas Roberts, Christina Chen, Swapnil V. Shewale, Peter Bell, Juliette Hordeaux, James M. Wilson

P58 **Histologic Method for Nonhuman Primate Tooth Evaluation on Toxicity Studies**
Sarah Coe, Rachel Stoops, Chris Bollinger, Deanna Buford, Matthew Zipprich, Susan Kent, Judit Markovits

P59 **Refreshed ICR Mouse Colony to Eliminate Retinal Degeneration Associated with pde6b Mutation**
Sarah Coe, Jaymie Voorhees, Charlotte Hollinger, Sheri Church

P60 **Comparative Short-Term (5-day) *In Vivo* Repeat Dose Biological Potency Studies of Five *Ginkgo biloba* Extract Lots in Male F344/NCrl Rats: Selected Apical, Clinical Pathology and Toxicogenomic Results**
Michelle C. Cora, Cynthia V. Rider, Frederick Parham, Suramaya Waidyanatha, Georgia K. Roberts, Kelly A. Shipkowski, Scott S. Auerbach

P61 **Spontaneous Cardiomyopathy in Mauritian-Source Compared to Asian-Source Cynomolgus Macaques: Incidence and Characterization**
Joshua H. Decker, Lydia L. Andrews-Jones, Wayne R. Buck, Stacey L. Fossey, Shima Mehrvar, Michele R. Phillips, Tatiana A. Sharapova, David Rehagen, Kevin O. Maisonave, Edyta Jarmulkowicz, Magali R. Guffroy

P62 **Feline Valvular and Mural Eosinophilic and Granulomatous Endomyocarditis (Feline Hypereosinophilic Syndrome) with Congestive Heart Failure**
Paulina Gomez, Jessica Ward, Elizabeth Mason, Olufemi Fasina

P63 **Spontaneous Cardiac Findings in Research Colony Cynomolgus and Rhesus Macaques: A 3-Year Survey**
Jiashi Feng, Sarah Coe, Nicholas Vetter

P64 **Procedural-Related Microscopic Observations in Rats with Indwelling Intravenous Catheters in Nonclinical Toxicology Studies**
Sarai Milliron, Sherry Morgan

P65 **Toxicologic Evaluation of RC-0315, a Mesenchymal Stem Cell-Derived Secretome, Following Repeated Intratracheal Administration in Mice**
Michael Timaner, Tali Fishman-Jacob, Michal Steiner, Noam Kronfeld, Abraham Nyska, Yuval Ramot

P66 **Preliminary Studies for Neurotoxicity from Intranasal Exposure of Zinc Oxide Nanoparticles in APOE3 and APOE4 Humanized Mice**
Jesse Riker, Shaolin Liu

P67 **Retrospective Study of Infectious Cardiac Lesions in Old and New World Nonhuman Primates: Morphologic Spectrum, Etiologies, and Implications for Toxicologic Pathology**
Vinay Shivanna, Donna Perry, Edward Dick, Olga Gonzalez

P68 **Chronic Arteriovenous Fistula/Shunt in the Pelvic Limb of a Naïve Peripubertal Cynomolgus Monkey (*Macaca fascicularis*)**
Vanessa Vrolyk, Laura Neagu-Lund, Marie-Josée Desmarais

P69 **Distinguishing Disease-Associated from Test Article-Related Thrombocytopenia in a SHIV-Infected Rhesus Macaque Following AAV-Delivered HIV-1 IgG Therapy**
Rachael Wolters, Altair Fazio, Philip Barnette, Tracy Ordonez, Monica Shroyer, Ann Hessell, Nancy Haigwood, Mauricio Martins

P70 **Results of the 2026 Membership-Wide Survey on the Topics of Diversity, Inclusion and Belonging in the Society of Toxicologic Pathology**
Agathe Bedard, Christina Alarcón

Abstracts

P01 Utility of Immunohistochemical Characterization of Prechronic Lung Lesions as Early Markers of Chemical-Induced Carcinogenesis in Rodent Toxicology Studies

Mallikarjun Bidarimath, Mark F. Cesta, Robert C. Sills, Sonika Patial

Comparative and Molecular Pathogenesis Branch, Division of Translational Toxicology, National Institute of Environmental Health Sciences, Durham, NC, USA

Abstract

INTRODUCTION: Two-year rodent bioassays are the standard for assessing lung carcinogenicity but are costly and time-consuming, highlighting the need for shorter-term approaches. Comparing 90-day lung lesions with 2-year tumor outcomes identified three prechronic lesion-tumor patterns: 1) hyperplasia/inflammation and tumors; 2) hyperplasia/inflammation but no tumors; and 3) no hyperplasia/inflammation but tumors, suggesting histopathology alone may not capture early tumorigenic events. We hypothesized that immunohistochemical biomarkers may facilitate early identification of carcinogenic potential.

EXPERIMENTAL DESIGN: Mouse lung lesions from 90-day studies representing three prechronic lesion-tumor patterns: Indium phosphide, 2,3-Butanedione, and Cumene were analyzed by immunohistochemistry.

METHODS: Immunohistochemistry was used to assess inflammation (CD45, COX-2), proliferation (Ki-67), stress/DNA damage (p53), and epithelial differentiation (CC10, SP-C). Staining was scored semiquantitatively (minimal to marked).

RESULTS: Indium phosphide increased CD45 (mild–moderate), COX-2 (marked), Ki-67 (mild), p53 (moderate–marked), and CC10 (marked) immunoreactivity, with decreased SP-C, consistent with robust inflammation, increased cell turnover/stress, and altered epithelial differentiation. In contrast, 2,3-butanedione increased CD45 (mild–moderate), COX-2 (mild), Ki-67 and p53 (minimal), and CC10 (mild) immunoreactivity, with no change in SP-C, suggesting a transient response with mild inflammation, limited proliferation, and preserved differentiation. Cumene showed minimal to no changes in these markers despite tumor formation.

CONCLUSION: Marked inflammation, proliferation, and altered differentiation were associated with tumors (indium phosphide), whereas milder responses were not (2,3-butanedione). Tumors also occurred without early biomarker changes (cumene), indicating mechanistic heterogeneity.

IMPACT STATEMENT: Immunohistochemical profiling in subchronic studies adds mechanistic resolution beyond histopathology, distinguishing chemicals with similar prechronic lesions but different tumor outcomes.

P02 Chronic Liver Toxicity Promotes Liver Fibrosis by Hepatocyte Dedifferentiation into Myofibroblast-Like Cells Through the TGF-β1-Oct4 Axis

Manisha Yadav[1,2], Shobhit Verma[1,2], Smriti Verma[1,2], Madhav Nilakanth Mugale[1,2]

[1] Toxicologic & Experimental Medicine, CSIR-Central Drug Research Institute, Lucknow, Uttar Pradesh, India. [2] Academy of Scientific and Innovative Research (AcSIR), Ghaziabad, Uttar Pradesh, India.

Abstract

OBJECTIVE: Chronic toxicity promotes hepatocyte dedifferentiation toward a myofibroblast-like phenotype, which remains unclear. The present study aimed to investigate the role of stemness-associated transcription factors, particularly Oct4, in fibrosis remodelling using integrated *in vitro* and *in vivo* approaches.

EXPERIMENTAL DESIGN: Male Sprague-Dawley rats were divided into 2 groups (N=36): control (n = 18) and Thioacetamide (TA)-induced (n=18). Liver fibrosis was induced by intraperitoneal TA (150 mg/kg) thrice weekly for up to 12 weeks. Animals were sacrificed at 4, 8, and 12 weeks for the longitudinal assessment. In parallel, *in vitro* studies were conducted in TA-treated HepG2 cells, with pharmacological inhibition of TGF-β1 and Oct4 to evaluate their functional roles.

METHODOLOGY: Liver sections were analysed by histological (H&E, Masson's trichrome, and picrosirius red), immunohistochemistry, and immunofluorescence techniques. Biochemical, antioxidant assays, and hydroxyproline content. *In vitro* immunofluorescence was performed to assess marker expression.

RESULTS: Chronic toxicity leads to progressive liver injury, activation of inflammatory markers, and marked inflammation, collagen deposition, and fibrosis. Oxidative stress was evident from increased NOX2 and MDA levels, accompanied by reduced antioxidant levels. Activation of TGF-β1/pSmad2/3 signalling was observed. Hepatocytes exhibited increased Oct4, Runx2, and Sox9, alongside reduced albumin and HNF4α, indicating loss of hepatocyte identity and acquisition of myofibroblast-like features (α-SMA, collagen I). Inhibition of TGF-β and Oct4 attenuated fibrotic responses in *in vitro*.

CONCLUSION: TA-induced hepatotoxicity drives hepatocyte plasticity through TGF-β1-mediated signaling, revealing a novel mechanistic link between toxic injury and fibrosis progression.

IMPACT STATEMENT: These findings suggest future therapeutic strategies in toxicologic pathology/Liver fibrosis.

P03 Hsd17b7 Is Required for Proper Mammalian CNS Development

Bayla Bessemer[1,2], *Rolf Stottmann*[2,3]

[1]The Ohio State University College of Veterinary Medicine, Columbus, OH, USA. [2]Nationwide Children's Hospital, Institute of Genomic Medicine, Columbus, OH, USA. [3]The Ohio State University Department of Pediatrics, Columbus, OH, USA

Abstract

Disorders of cholesterol biosynthesis are genetic diseases that can have life-threatening impacts on early development. Clinical features include intellectual disability, craniofacial developmental anomalies, and a range of cerebral and cerebellar malformations. Hydroxysteroid 17-Beta Dehydrogenase 7 (Hsd17b7) is a gene which encodes for a post-squalene cholesterol biosynthesis enzyme. The objective of this study is to investigate the consequences of complete Hsd17b7 deletion on the CNS. Whole embryo ablation of Hsd17b7 is embryonically lethal early in development. To overcome this, we have utilized mouse Cre-LoxP systems to ablate Hsd17b7 from the neural crest using Wnt1cre2 and the forebrain with Emx1cre. Phenotypes in mutant mice are characterized through gross examination, histology, skeletal preps, immunohistochemistry, and behavioral assays. Mechanisms are then investigated with fluorescent reporter cre mT/mG, wholemount IHC, and in situ hybridization. Replicate number is determined through *a priori*. Wnt1Cre2/Wt;Hsd17b7Flox/Wt mice reveal cerebellar dysgenesis linked to changes in the midbrain-hindbrain boundary, midbrain hypoplasia, severe hydrocephaly linked to malformation of the subcomissural organ, and craniofacial anomalies. Emx1Cre/Wt;Hsd17b7Flox/Wt mice have a severely hypoplastic forebrain. We suspect that loss of Hsd17b7 in the Wnt1cre2 mice leads to early apoptosis of the Wnt1 lineage, directly compromising development of the cerebellum and the craniofacial primordia. Loss of Hsd17b7 in Emx1cre mice is anticipated to hinder smoothened function through decreasing access of cholesterol, inhibiting proper hedgehog signaling. We show that the gene Hsd17b7 is required for proper CNS development; a more comprehensive understanding of how disruptions of the cholesterol biosynthesis pathway impacts fetal development offers an opportunity to develop more effective therapeutic strategies.

P04 Sectional and Transmural Variation in Ultrastructural Morphology of the Left Ventricle in Canine Primary Dilated Cardiomyopathy

Mark D. Bilger[1,2], *Lisa Freeman*[2]

[1]University of Wisconsin, Madison, WI, USA. [2]Tufts Cummings School of Veterinary Medicine, North Grafton, MA, USA

Abstract

Transmission electron microscopy (TEM) is a valuable tool for investigating cardiomyocyte ultrastructure in animal models of myocardial disease. Differences in mitochondrial size have been reported in humans with primary dilated cardiomyopathy (DCM) and dogs with experimentally-induced heart failure compared to healthy patients. Ultrastructural morphological differences have been previously reported transmurally and between heart chambers in healthy dogs, but similar TEM studies examining transmural and regional morphology in humans or dogs with primary DCM are lacking. Hearts from five dogs with primary DCM were examined with TEM. Sections from the lateral and posterior left ventricular free wall were compared across the subepicardial, mid-myocardial, and subendocardial levels of the myocardium and for the interfibrillar, perinuclear, and subsarcolemmal regions of the cardiomyocyte. Compared to the mid-myocardium, mitochondria in the sub-epicardium were significantly smaller in the interfibrillar (P=0.014) and subsarcolemmal (*P*=0.035) regions of the cardiomyocyte. There was no significant difference in mitochondrial stage across myocardial levels and no significant differences in mitochondrial size or stage between sections. There are significant differences in mitochondrial size across different levels of the heart. Subendocardial or mid-myocardial left ventricular tissue may be more representative of average mitochondrial size in dogs with primary DCM. Regional differences in mitochondrial size may impact interpretation of TEM studies in dogs with primary DCM. Details on heart section, level, and region are valuable to report in TEM studies.

P05 MRP4 Modulates Hepatic Response to Phenobarbital by Regulating Proliferative and Metabolic Pathways

Ankit P. Laddha, Hangyu Wu, José E. Manautou

Department of Pharmacy and Pharmaceutical Sciences, University of Connecticut, Storrs, CT, USA

Abstract

BACKGROUND AND PURPOSE: Membrane transporters are essential for hepatic homeostasis by mediating the movement of endogenous metabolites and xenobiotics. The Multidrug Resistance Protein 4 plays a key role in hepatic adaptation to chemical stress. We previously showed that MRP4 expression increases following acetaminophen exposure and localizes to proliferative regions. Although MRP4 deficiency did not impair proliferation after partial hepatectomy, it promoted hepatic steatosis. Here, we investigated its role in hepatocyte growth and metabolic remodeling using a phenobarbital-induced hepatomegaly model.

METHODS: Wild-type and Mrp4$^{-/-}$ mice were treated with phenobarbital (50 or 100 mg/kg, 10 days). Liver growth, injury, histology, proliferation (Ki67), triglycerides, and lipid accumulation (Oil Red O) were assessed. Gene and protein expression were analyzed by qPCR and immunoblotting. Global proteomic analysis was performed to identify altered biological pathways.

RESULTS: Mrp4$^{-/-}$ mice showed increased liver-to-body weight ratios and elevated ALT levels, indicating enhanced hepatomegaly and injury. Histology revealed hepatocellular hypertrophy with increased mitotic figures. Proliferation markers (Pcna, Cdk1/2, Cyclin B1, c-Myc) and xenobiotic genes (Cyp2b10, Cyp3a11, Cyp2c29) were upregulated, while Cyp7a1 and Cyp2e1 were downregulated. Increased phosphorylation of cAMP Response Element-Binding Protein with reduced Salt Inducible Kinase 2 suggests CREB activation. Lipid genes (Lpl, Pparγ, Dgat1, Acot2) were elevated, whereas Fasn and Acc were reduced, consistent with lipid accumulation. Proteomics revealed enrichment of pathways related to cell cycle signaling, mitochondrial metabolism, and lipid dysregulation.

CONCLUSION: MRP4 deficiency amplifies phenobarbital-induced hepatic growth and metabolic remodeling, indicating an indirect role in modulating proliferative signaling through metabolic and detoxification pathways.

P06 Loss of Brain Resilience with microRNA-29 Reduction in the Context of Alzheimer's Disease

Jonathan Nagel, Nazanin Kiapour, Keeley Spiess, Sheryl Moy, Mohanish Deshmukh

University of North Carolina, Chapel Hill, NC, USA

Abstract

INTRODUCTION: microRNA-29 (miR-29) is vital to mature brain homeostasis, and reduced levels of miR-29 in the brain have been associated with Alzheimer's disease (AD). While miR-29 offers a potential avenue of AD therapy, the effects of miR-29 reduction in the brain are not entirely understood.

OBJECTIVES: We aim to: 1) Define the changes in miR-29 levels in multiple murine models of AD; 2) Evaluate the effects of reduced miR-29 in the neurons of adult wild type mice.

METHODS: 1) We measured brain miR-29 levels (qRT-PCR) in three murine AD models: APP/PS1, PS19, N-L-GF; 2) We created a cre/lox mouse model to induce knock-out of miR-29 in Thy1-positive neurons at 4 months of age. These mice were evaluated for survivability, gene expression changes, behavioral abnormalities, and AD-associated lesions.

RESULTS: 1) Brain miR-29 was reduced by up to 50% in the tested AD murine models; 2) While partial deletion of miR-29 did not affect survivability, complete deletion resulted in premature lethality. miR-29 deletion also resulted in behavioral disinhibition, decreased seizure threshold, and altered expression of several AD-associated genes (e.g. NAV3).

CONCLUSIONS: 1) miR-29 levels are reduced in several established AD mouse models; 2) miR-29 expression in neurons is vital to brain homeostasis, and reduced miR-29 likely plays a role in AD pathogenesis.

IMPACT STATEMENT: The links between miR-29 and AD shown here further support miR-29 as a promising AD treatment. Future directions include evaluation of AAV gene therapy to restore endogenous levels of miR-29 in the brains of AD model mice.

P07 Can You Identify Hepatic Sinusoidal Lining Cells On HE Sections?

Hinata Niimi, Mitsuru Kuwamura, Takeshi Izawa

Osaka Metropolitan University, Izumisano, Osaka, Japan

Abstract

INTRODUCTION: This study investigated whether hepatic sinusoidal lining cells—Kupffer cells, hepatic stellate cells, and sinusoidal endothelial cells—can be identified solely on hematoxylin and eosin (HE)-stained sections. In addition, we evaluated whether identification of these cells becomes easier under specific toxicological conditions.

EXPERIMENTAL DESIGN: Formalin-fixed paraffin-embedded blocks of the liver were collected from saline-treated (control), lipopolysaccharide (LPS)-treated, and thioacetamide treated F344/DuCrlCrlj rats. HE sections were digitally scanned at 40× magnification using an Olympus VS-120. After scanning and removing cover glasses, the sections were subjected to immunohistochemistry (IHC) for Iba-1 (Kupffer cells), GFAP (stellate cells), and von Willebrand factor (vWF; endothelial cells). IHC-stained sections were rescanned and the whole slide images of HE and IHC were compared at identical locations on the same slides.

RESULTS: In control livers, morphologies of hepatic sinusoidal lining cells are generally similar. If anything, Kupffer cells exhibited various nuclear morphologies, including club-shaped, comma-shaped, and round forms. Stellate cells commonly showed short rod-shaped nuclei. Sinusoidal endothelial cells were observed as elongated, spindle-shaped thin nuclei lining sinusoids. In the LPS-treated liver, Kupffer cells appeared mildly enlarged and more rounded compared with controls.

CONCLUSION: Under normal conditions, distinguishing of hepatic sinusoidal lining cells is usually difficult due to their similar nuclear morphology. IHC would increase accuracy when toxicological pathologists evaluate specific sinusoidal lining cells for consideration of toxicological mechanism.

IMPACT STATEMENT: It is difficult to identify hepatic sinusoidal lining cells solely based on HE morphology.

P08 Autopsy-Based Evidence of Early Hepatocellular Injury in Fatal Glyphosate Poisoning in a 16-Year-Old Girl

Mrinal Patnaik[1], Poonam Patnaik[2]

[1]All India Institute of Medical Sciences, Raipur, Chhattisgarh, India. [2]Jamia Millia Islamia, New Delhi, Delhi, India

Abstract

Glyphosate-based herbicides are widely used agrochemicals traditionally regarded as having low human toxicity, however, severe and fatal outcomes continue to be reported, particularly following ingestion of concentrated formulations. We present an autopsy case of a 16-year-old female who was brought dead following deliberate ingestion of a glyphosate-containing herbicide.

The decedent was reportedly asymptomatic prior to the ingestion and developed mild headache, several episodes of vomiting and sudden deterioration culminating in death before medical intervention could be instituted. Medico-legal autopsy was performed the following day after overnight refrigerated storage. Gross examination revealed generalized visceral congestion with no specific focal pathology. Histopathological examination of the liver demonstrated prominent hepatocellular ballooning degeneration with cytoplasmic rarefaction, consistent with acute toxic hepatopathy. Mild periportal inflammatory infiltrates and sinusoidal dilatation was seen. No significant steatosis, fibrosis was noted.

Glyphosate formulations are known to produce multi-system toxicity, including metabolic acidosis, renal impairment, pulmonary edema, and cardiovascular instability, often progressing to shock and death within 12–72 hours in severe cases. Proposed mechanisms include disruption of cellular and mitochondrial membranes and uncoupling of oxidative phosphorylation, largely attributed to surfactant co-formulants rather than glyphosate alone. Early hepatic injury, as evidenced by ballooning degeneration, likely reflects cytoskeletal disruption and intracellular fluid shifts secondary to toxic insult.

This case highlights importance of detailed histopathological evaluation in suspected poisoning deaths. Occurrence of significant hepato-cellular injury even in rapidly fatal poisoning and recognition of such findings contributes to a better understanding of pathophysiological mechanisms underlying sudden death in acute herbicide toxicity.

P09 Microscopic Nomenclature Used in Evaluation of Nonnclinical Wound Healing Studies: Highlighting Gaps in Current INHAND Terminology

Elise M. Peauroi[1,2], Sarah Davis[1], Lyn M. Wancket[1]

[1]Charles River Laboratories, Mattawan, MI, USA. [2]Michigan State University Veterinary Diagnostic Laboratory, Lansing, MI, USA

Abstract

While the International Harmonization of Nomenclature and Diagnostic Criteria for Lesions (INHAND) initiative has established globally standardized nomenclature for toxicologic pathology evaluations, there is no harmonized language available for the microscopic evaluation of non-clinical medical device studies. These studies incorporate unique categories of pathologic findings that are not well represented by current INHAND diagnoses, including specific terms for wound healing and tissue reactions to device materials. An international working group is currently addressing medical device nomenclature; in the interim, we investigated terms used in 19 skin wound healing studies conducted at one contract research organization (CRO) and evaluated microscopically by 10 different pathologists at two CROs. Diagnostic terms, locators and modifiers were tabulated and categorized by data capture method (free text in Excel vs validated data capture system Provantis); whether severity scores or present/absent schemes were used; and whether the term was currently included in INHAND nomenclature (with or without modification of the definition). The terms used by pathologists varied by study design and data capture method. Some of the most frequently used term categories were absent or heavily modified from INHAND, particularly those describing normal components of the wound healing process, including epithelialization, granulation tissue and seroma. This work reveals the lack of concordance among pathologists and the absence of key healing-related terms in the INHAND nomenclature, underscoring the importance of the development of standardized guidance for the use of language in non-clinical evaluation of medical devices.

P10 An Indian Traditional Medicine – Vasant Kusumakar Rasa Ameliorates Renal Damage in Diabetic Rats

Alok D. Singh[1], Mukesh B. Chawda[2], Yogesh A. Kulkarni[1]

[1]Shobhaben Pratapbhai Patel School of Pharmacy & Technology Management, SVKM's Narsee Monjee Institute of Management Studies (NMIMS) Deemed to be University, Mumbai, Maharashtra, India. [2]Shree Dhootapapeshwar Limited, Mumbai, Maharashtra, India

Abstract

INTRODUCTION: Diabetic nephropathy is a complication of diabetes that adversely affects renal health. Vasant Kusumakar Rasa (VKR) is a traditional formulation reported in Ayurveda for diabetes management. The present research work aimed to assess the efficacy of VKR in a rodent model that reflects the pathophysiological characteristics of type 2 diabetic nephropathy.

EXPERIMENTAL DESIGN: The male Sprague-Dawley rats were fed with high fat diet for 2 weeks followed by administration of single dose of streptozotocin (35 mg/kg, *i.p.*). After confirmation of diabetes, animals were treated with VKR at dose (28 and 56 mg/kg, *p.o.*) for the next 16 weeks.

MATERIALS & METHODS: Biochemical parameters, renal function, inflammatory markers, oxidative stress indicators were estimated. Histopathology of kidney tissue using haematoxylin and eosin, periodic acid-Schiff, and Masson's trichrome was also carried out. Changes of TGF-β1 and Smad2/3 protein were determined with western blot analysis.

RESULTS: VKR effectively lowered levels of biochemical parameters in blood and urine samples. Kidney tissue analysis indicated a decrease in pro-inflammatory mediators and antioxidant enzyme markers post-VKR treatment. Histopathology showed reduced degenerative changes in treatment groups compared to the diabetic control. Western blotting indicated significant TGF-β1 and Smad2/3 downregulation after 16 weeks of VKR treatment.

CONCLUSION: The study substantiates that VKR exerts a considerable positive role in the management of type 2 diabetic nephropathy in experimental rat model.

IMPACT STATEMENT: Vasant Kusumakar Rasa demonstrates its potential as a complementary therapeutic strategy to mitigate the effects of type 2 diabetic nephropathy in rats.

P11 Identification of Disease-Associated Polyomaviruses from Cynomolgus Macaques Undergoing Stem Cell Transplantation

Helena Vogel[1], *Tristan T. Neal*[1], *Helen L. Wu*[2], *Paul Kievit*[2], *Jonah B. Sacha*[2], *Gabriel J. Starrett*[1]

[1]NIH NCI, Bethesda, MD, USA. [2]ONPRC, Beaverton, OR, USA

Abstract

BK polyomavirus reactivation and associated hemorrhagic cystitis/nephropathy is a significant cause of morbidity following solid organ or hematopoietic stem cell transplantation (HSCT) in humans, yet therapeutic options remain limited. Mauritian cynomolgus macaques (MCM), a key nonhuman primate species in toxicologic pathology, exhibit similar post-transplant complications, making them a valuable spontaneous disease model. To characterize the urinary DNA virome and the viruses associated with cystitis/nephritis, we performed deep sequencing of urine from both HSCT-recipient and healthy MCM.

Our analysis demonstrated distinct urinary virome compositions, with polyomaviruses predominating in HSCT recipients and bacteriophages predominating in healthy controls. Three polyomaviruses were identified with apparent host tropism for cynomolgus macaques: *Macaca fascicularis* polyomavirus 2 (MafaPyV2), *Macaca fascicularis* polyomavirus 3 (MafaPyV3), both closely related to human polyomaviruses, and a newly characterized simian virus 40 strain (SV40 typeIIB). All three viruses were detected in the urine of both transplanted and healthy animals but were shed at significantly higher relative loads in HSCT recipients. Specifically, the majority of HSCT recipients with abundant shedding presented with urologic disease. All three polyomaviruses were shed in the urine of animals with urologic disease, with a predominance of MafaPyV2, while SV40 type IIB was the predominant polyomavirus shed in healthy MCM.

These findings closely parallel human transplant-associated viral reactivation, urine virome composition, and associated complications. This robust, translationally relevant model of spontaneous viral disease offers a critical platform for evaluating antiviral therapies and underscores the importance of recognizing this naturally occurring pathology as a potential confounder in safety assessments.

P12 Modeling Th2-Driven Pathogenesis of Atopic Dermatitis Using Canine Primary Epidermal Organoids

Bo Chen[1,2], *Ron Slocombe*[1], *Yuanting Zheng*[3], *Mirjana Bogeski*[1], *Oluwadamilola Samuel Omotainsea*[1], *Smitha Rose Georgy*[1]

[1]Section of Anatomic Pathology, Melbourne Veterinary School, Faculty of Science, University of Melbourne, Werribee, VIC, Australia. [2]Department of Pathology, WuXi AppTec (Suzhou) Co., Ltd., Suzhou, Jiangsu, China. [3]Melbourne Veterinary School, Department of Veterinary Biosciences, Faculty of Science, University of Melbourne, Parkville, VIC, Australia

Abstract

INTRODUCTION/OBJECTIVES: Atopic dermatitis (AD) is a chronic inflammatory skin disease affecting humans and dogs, with canine AD (CAD) affecting 3-15% of dogs and causing significant discomfort. A longstanding question is whether epidermal barrier dysfunction or immune dysregulation initiates clinical disease. This study aimed to dissect how Th2 cytokines (IL-4 and IL-13) affect the epidermal barrier at morphologic and molecular levels using canine epidermal organoids.

METHODS AND MATERIALS: A well-controlled model of canine primary epidermal organoids (cPEOs) derived from normal keratinocytes was used.

EXPERIMENTAL DESIGN: First, the impact of IL-4 and IL-13 on the skin barrier was examined using cPEOs with/without Th2 cytokines via light microscopy and immunohistochemistry. Second, RNA sequencing compared treated to untreated cPEOs. Third, the Th2-conditioned model was used to examine the JAK1 inhibitor oclacitinib and investigate potential downstream roles for JAK1, STAT3, and STAT6.

RESULTS: Th2 cytokine treatment induced AD-like features, including epidermal spongiosis and reduced suprabasal differentiation. Transcriptomics identified 224 differentially expressed genes. Pathway analyses showed immune activation and suppression of differentiation, keratinization, and lipid metabolism. Oclacitinib partially restored Th2-induced differentiation deficits.

CONCLUSION: This work establishes an innovative *in vitro* model recapitulating key features of atopic skin, providing a gene-level framework for mechanistic studies and validating a translational platform for Th2-axis therapeutics.

IMPACT STATEMENT: This canine epidermal organoid model bridges 2D cell culture and animal studies, offering a valuable tool for investigating disease mechanisms and evaluating therapeutics while underscoring the need for individualized therapy in CAD and informing comparative approaches for human AD.

P13 From Constraints to Capability: Developing a User-Friendly Deep Learning Framework in a Cost-Constrained Research Environment

Brian R. LaMendola, Rachael M. Wolters, Altair E. Fazio, Nathan P. Crilly

Oregon Health and Science University, Beaverton, OR, USA

Abstract

INTRODUCTION: The integration of artificial intelligence (AI)-driven image analysis into histopathologic evaluation has expanded rapidly, driven by increasing expectations for objective, quantitative endpoints. However, access to user-friendly commercial platforms (e.g., HALO, Aiforia) is often limited in cost-constrained research environments, creating barriers for pathologists seeking to adopt AI-based methods. Here, we describe an AI-driven image analysis framework for multiclass histology object classification using open-source tools, minimizing the need for advanced computational expertise, expensive software, or specialized hardware.

METHODS: We reviewed available image analysis tools for applicability and ease of use. We then established a framework utilizing QuPath for image annotation and dataset preparation, followed by training a supervised, machine-learning model using StarDist for object detection and segmentation, with step-by-step guidance for users with minimal computational backgrounds. To evaluate the usefulness of our framework, we developed a supervised machine-learning model to quantify lipidotic hepatocytes in a primate model of nonalcoholic steatohepatitis (NASH).

RESULTS: The final framework is streamlined and can be implemented and adapted by users with minimal computational expertise. Our resulting model performance is promising and continues to improve with refinement.

CONCLUSION: We successfully developed and implemented an open-source framework for multiclass histology object detection, used to quantify lipidotic hepatocytes in NASH. This highlights a feasible pathway for implementing AI-based image analysis in resource-limited settings and underscores the potential for open-source tools to meet growing demands for quantitative pathology.

IMPACT STATEMENT: This work demonstrates that cost-effective, open-source AI solutions can bridge the gap between rising analytical expectations and limited resources.

P14 A Two-Phase Validation Framework Informed by an *In Vitro* Cardiotoxicity Screening Case Study

Yigunag Zhu[1], Kathleen Gabrielson[2], Mark Kohr[1], Vasiliki Machairaki[3,4], Lena Smirnova[1,5], Paul A. Locke[1]

[1]Department of Environmental Health and Engineering, Bloomberg School of Public Health, Johns Hopkins University, Baltimore, MD, USA. [2]Department of Molecular and Comparative Pathobiology, Johns Hopkins University School of Medicine, Baltimore, MD, USA. [3]Department of Genetic Medicine, Johns Hopkins University School of Medicine, Baltimore, MD, USA. [4]The Richman Family Precision Medicine Center of Excellence in Alzheimer's Disease, Johns Hopkins University School of Medicine, Baltimore, MD, USA. [5]Center for Alternatives to Animal Testing (CAAT), Whiting School of Engineering, Johns Hopkins University, Baltimore, MD, USA

Abstract

INTRODUCTION: Off-target cardiotoxicity remains a major challenge in drug development. New Approach Methods (NAMs), including complex *in vitro* models, provide mechanistic and human-relevant approaches for earlier identification of cardiac safety liabilities. However, regulatory acceptance remains limited because current validation practices often impose a narrow context-of-use (CoU) upfront, restricting their broader applications. To address this bottleneck, we developed and evaluated a two-phase validation framework that separates foundational scientific validation from subsequent CoU qualification, supporting a broader verification process for regulatory application.

METHODS AND MATERIALS: In the validation phase, a human induced pluripotent stem cell-derived cardiac organoid-based cardiotoxicity screening model was evaluated using morphological, electro-mechanical, and transcriptional endpoints. These data were compiled into a validation data package documenting model performance, limitations, and potential applications. In the qualification phase, the model was assessed for the defined CoU: drug-induced proarrhythmic risk screening.

RESULTS: In the validation phase, biological relevance and technical characterization established baseline reliability across key assay endpoints. In the qualification phase, the model captured drug-induced phenotypes consistent with known proarrhythmic risk profiles of reference compounds. Separating validation from qualification also enabled clearer identification of model limitations and applicability domains without prematurely restricting future uses of the model.

CONCLUSION: Decoupling scientific validation from CoU qualification preserved model versatility while supporting focused regulatory decision-making for cardiovascular safety applications. This approach could accelerate the acceptance of life-saving therapeutics.

IMPACT STATEMENT: This framework provides a practical strategy to integrate NAMs, including cardiac organoid models, into toxicologic pathology and regulatory safety assessment.

P15 Spatiotemporal Analyses of Early Hepatocarcinogenesis Reveal Liver-Resident ILC1s as a Major Player in Early Immune Surveillance

Patrick Huang[1,2], Rajiv Trehan[1,3], Benjamin Ruf[4], Chi Ma[1], Dana Soika[1], Lorenz Kocheise[1], Gabriel Bacil Prata[1], Tim Greten[1], Firouzeh Korangy[1]

[1]National Cancer Institute, National Institutes of Health, Bethesda, MD, USA. [2]Purdue University College of Veterinary Medicine, West Lafayette, IN, USA. [3]Baylor College of Medicine, Houston, TX, USA. [4]University of Tübingen, Tübingen, Germany

Abstract

Hepatocellular carcinoma (HCC) is a frequent outcome of chronic liver injury and a common focus of preclinical comparative pathology models. There is a lack of studies defining the dynamic roles of immune cells during the earliest phases of tumor initiation. Our objective was to construct an immune atlas of early tumorigenesis, focusing on innate lymphoid cells (ILCs) and innate-like T cells (ILTCs) to understand their mechanisms in hepatic tumor initiation and progression.

We utilized a plasmid-induced (MYC-Luc;sg-p53) murine HCC model to evaluate temporal shifts in immune populations. Dysplastic cellular changes within hepatocytes were observed as early as day 4 post-injection of plasmids, during which most ILC and ILTC populations, including mucosal-associated invariant T (MAIT) cells, group 1 ILCs, ILC2s, and ILC3s, expanded in frequency. Depletion of liver-resident Hobit-expressing ILC1s resulted in a significant increase in early tumor burden, highlighting their role as pivotal effectors of anti-tumor immunity. Transcriptional and cytokine profiling identified tumor-derived IL-15 as an early mediator and activator of hepatic ILC1s. Crucially, multiplex immunohistochemistry demonstrated the spatial architecture of this response, localizing ILC1s directly within the microenvironment of early dysplastic liver lesions in both mice and humans. Therefore, ILCs and ILTCs are rapid responders to hepatic oncogenic transformation, with the IL-15-ILC1 axis acting as a mechanism of early anti-tumor defense.

Characterizing this spatiotemporal immune atlas during early hepatocarcinogenesis provides comparative pathologists with critical mechanistic data for evaluating immunomodulatory therapeutics and understanding spontaneous or induced hepatic neoplastic lesions in preclinical models.

P16 A Novel TGFβ Pathway Reporter Mouse Reveals Stage-Specific Suppression of Mitochondrial Metabolism in Mammary Tumorigenesis

Zachary Millman[1,2], Lalage Wakefield[1], Yu-an Yang[1]

[1]National Cancer Institute, National Institutes of Health, Bethesda, MD, USA. [2]Michigan State University, East Lansing, MI, USA

Abstract

Despite decades of research and numerous clinical trials, no FDA-approved TGFβ antagonists exist for cancer. This failure reflects the pleiotropic nature of TGFβ in tumorigenesis, where it suppresses tumor growth early while promoting invasion and extracellular matrix remodeling in later stages. We hypothesize that a fundamental barrier to therapeutic success is our inability to resolve which cells respond to TGFβ and how. To address this, we developed a TGFβ pathway reporter ("Lime") mouse with a Smad3-responsive GFP reporter that labels cells with active TGFβ signaling (S3x6>eGFP). To investigate how TGFβ responses evolve during tumorigenesis, we intercrossed this reporter with the MMTV-PyMT mouse and performed single-cell RNA-sequencing with matched GFP immunohistochemistry on mammary glands and tumors across normal, pre-neoplastic, and late tumor stages, with and without dual TGFβ antagonism using galunisertib and 1D11 (n = 4 mice/group). TGFβ antagonism partially reversed the tumor cell transcriptome toward a pre-neoplastic state, and GSEA identified enrichment of oxidative phosphorylation (NES = 2.2), ATP biosynthetic process (NES = 2.6), and mitochondrial respiratory chain complex I assembly (NES = 2.4) signatures. Western blot analysis of PyMT tumor cells confirmed that chronic TGFβ treatment depletes mitochondrial protein complexes *in vitro*. These findings indicate that TGFβ suppresses mitochondrial metabolism in tumor cells, and that its blockade restores oxidative phosphorylation, thus exposing a potential vulnerability to mitochondrial inhibitors. The LimePyMT reporter mouse provides a powerful tool for resolving cell type- and stage-specific roles of TGFβ in tumorigenesis, with direct implications for understanding therapeutic failure and developing combination strategies.

P17 Analyzing the Genetic Basis and Transcriptional Features of Sarcomas in Irradiated Rhesus Macaques

Courtney S. Moore[1], *Karl Dykema*[22], *Nury Steuerwald*[2], *Mark Cline*[1]

[1]Wake Forest University School of Medicine, Winston-Salem, NC, USA. [2]Atrium Health Levine Cancer Institute, Charlotte, NC, USA

Abstract

INTRODUCTION: Radiation-induced sarcomas (RIS) are rare tumors that occur in humans secondary to radiation exposures, most often radiotherapy. These neoplasms are aggressive and difficult to treat.

EXPERIMENTAL DESIGN: RIS were obtained from rhesus macaques that were previously irradiated via acute, total body, single dose, photon radiation (5 to 8.05 Gy, 4-7 years after exposure) and included four malignant nerve sheath tumors, one fibrosarcoma, one malignant glomus tumor, and one hemangiosarcoma. Spontaneous sarcomas (SS) occurred in four unirradiated rhesus macaques and were all malignant nerve sheath tumors.

METHODS: Snap frozen tumor samples (7 RIS, 4 SS) were analyzed by whole exome and RNA sequencing on an Illumina NextSeq 2000. Raw sequencing reads were processed and aligned to the Mmul_10 genome using nf-core sarek and nf-core rnaseq pipelines. Somatic variants, differential gene expression, and pathways (via Ingenuity Pathway Analysis) were evaluated.

RESULTS: In RIS to SS comparisons, missense mutations were the most abundant functional variant, single nucleotide polymorphisms were most prevalent, and C>T transitions were the primary single nucleotide class. Differentially up- and downregulated genes were enriched in neuronal, inflammatory, epidermal, and metabolic categories. Identified pathways highlighted roles in muscle formation, endothelial and neuronal function, and vascular integrity.

CONCLUSION: Whole exome sequencing revealed the mutation landscape was dominated by missense single nucleotide polymorphisms with a strong C>T transition signature, consistent with previously described mutational patterns in radiation-induced tumors.

IMPACT STATEMENT: RIS have identifiable genetic and transcriptomic signatures, which may guide future diagnostic and therapeutic strategies.

P18 Microplastic-Induced Cellular Toxicity: Effects on Connexin 43 and Connexin 26 Expression in Canine Mammary Cell Lines

Guilherme da Silva Rogerio[1,2], *Ivone Izabel Mackowiack da Fonseca*[3], *Maria Lúcia Zaidan Dagli*[3]

[1]Cancer Institute of The University of São Paulo (ICESP/USP), São Paulo, São Paulo, Brazil. [2]Laboratory of Comparative Oncology (LOEC/FMVZ), São Paulo, São Paulo, Brazil. [3]School of Veterinary Medicine - University of São Paulo (FMVZ/USP), São Paulo, São Paulo, Brazil

Abstract

INTRODUCTION: Microplastics are widespread environmental particles that vary in size, shape, and chemical makeup. Increasing evidence indicates that their accumulation in tissues can trigger biological responses, especially inflammatory processes. Additionally, microplastics may carry environmental contaminants, helping them enter cells and potentially disrupt cellular signaling and balance. Connexins, including Connexin 43 (Cx43) and Connexin 26 (Cx26), are essential components of gap junctions and play crucial roles in cell communication and tumor biology. Experimental Design and

METHODS: Two canine mammary cell lines were used: a normal mammary epithelial line (LOEC NMG) and a mammary adenocarcinoma line (LOEC MCA2). Cells were exposed to polystyrene microplastic particles (0.09–0.1 µm) at concentrations of 10 µg and 20 µg for 48 hours under sterile laminar flow conditions. After exposure, immunofluorescence analysis was performed to assess connexin expression. Cells were fixed with paraformaldehyde, permeabilized, and incubated in a blocking solution to reduce nonspecific binding. Samples were then treated with primary antibodies against Cx26 and Cx43, followed by fluorescent secondary antibodies. Nuclei were counterstained, and slides were mounted for fluorescence microscopy analysis.

RESULTS: No significant changes in connexin expression or cell shape were seen in the normal LOEC NMG cell line. In contrast, LOEC MCA2 cells showed early shape changes and redistribution of connexins toward the nuclear area after microplastic exposure.

IMPACT STATEMENT: These results suggest that microplastics may have toxic effects on cancerous mammary cells, altering connexin localization and possibly promoting tumor growth.

P19 Antileukemic Potential of Hydroalcoholic Extract of *Fagonia cretica* L. in Benzene-Induced Leukemia in Rats

Adeeba Zaidi, Nasreen Jahan

National Institute of Unani Medicine, Bengaluru, Karnataka, India

Abstract

INTRODUCTION/OBJECTIVES: *Fagonia cretica* L. is a medicinal herb traditionally used in various disorders, including cancer. This study aimed to evaluate the antileukemic potential of its hydroalcoholic extract in a benzene-induced leukemia model in rats.

METHODS AND MATERIALS: An acute oral toxicity study was conducted as per OECD guideline 423 to determine the safe dose. Male Wistar rats were used for evaluation of antileukemic activity.

EXPERIMENTAL DESIGN: Leukemia was induced by intravenous administration of benzene (0.2 mL) at 48-hour intervals for five weeks. Animals were divided into control, disease, test (140, 195, and 250 mg/kg extract), and standard (cyclophosphamide) groups. Treatment was continued for four weeks. Hematological parameters and peripheral blood smears were analyzed. Liver and spleen were collected for organ weight and histopathological evaluation.

RESULTS: The extract was found to be safe up to 5000 mg/kg. Benzene exposure resulted in significant anemia and leukocytosis ($p<0.05$) with abnormal leukocyte morphology. Treatment with *F. cretica* significantly improved hematological parameters and restored cellular morphology in a dose-dependent manner, with the highest dose showing effects comparable to cyclophosphamide.

CONCLUSION: The hydroalcoholic extract of *Fagonia cretica* demonstrated significant antileukemic activity in benzene-induced leukemia in rats.

IMPACT STATEMENT: These findings suggest that *Fagonia cretica* may serve as a potential plant-based therapeutic candidate for leukemia, warranting further mechanistic and clinical investigations.

P20 Severe Ocular Necrotizing Vasculopathy Following Suprachoroidal Delivery of a Polymeric Formulation in a Rhesus Macaque

Akhil A. Vinithakumar[1], Katharina M. Gregor[1], Mirella Rivera-Velazquez[2], Sarah E. Cook[3], Marie-Josee Marie-France Lemoy[2], Rebecca L. Sammak[2], Glenn Yiu[2,4], Katherine J. Olstad[1,2]

[1]California National Primate Center, University of California Davis, Davis, CA, USA. [2]Department of Pathology, Microbiology and Immunology, School of Veterinary Medicine, University of California Davis, Davis, CA, USA. [3]Comparative Pathology Laboratory, University of California Davis, Davis, CA, USA. [4]Department of Ophthalmology & Vision Science, School of Medicine, University of California Davis, Davis, CA, USA

Abstract

INTRODUCTION: Suprachoroidal (SC) injection is an emerging approach for targeted intraocular drug delivery that maximizes posterior segment exposure while minimizing systemic effects. While polymer-based vehicles offer potential for sustained release, their biocompatibility within SC space remains incompletely defined. This study characterizes acute clinicopathologic effects of a novel polymeric formulation following SC administration in a nonhuman primate (NHP).

EXPERIMENTAL DESIGN/METHODS: A 5-year-old intact female rhesus macaque (*Macaca mulatta*) received a poly lactic-co-glycolic acid-based formulation via SC injection (200 µL OD; 400 µL OS). The formulation was later determined to contain trace sodium dodecyl sulfate (~25 ppm). Clinical signs developed 1-day post-injection (PI), including bilateral periocular inflammation, mydriasis, visual impairment, hyphema, and inappetence. Opioid analgesia was started at injection. Antibiotics and immunosuppressive steroids were administered. Rapid clinical decline prompted humane euthanasia 2 days PI. Ocular tissues were collected for histopathologic and microbiologic evaluation.

RESULTS: Histopathologic changes centered on the uvea and consisted of diffuse necrotizing vasculopathy affecting small- and medium-sized vessels, characterized by fibrinoid necrosis, thrombosis, hemorrhage, fibrin exudation, and congestion, with extension and secondary lesions of adjacent tissues. Secondary lesions included retinal atrophy and stromal edema, hemorrhage, and inflammation. No infectious agents were identified.

CONCLUSION: Findings support an acute, severe uveal necrotizing vasculopathy associated with local SC exposure to polymeric formulation.

IMPACT STATEMENT: This case expands spectrum of ocular vascular injury in NHPs and highlights necessity of formulation- and excipient-aware safety evaluation for intraocular biomaterials and sustained-release drug delivery systems, as the SC space can mount severe, unintended vascular responses

P21 Treatment with Small-Molecule Biofilm Inhibitors in a Novel Murine Model of Chronic Typhoid Fever

Allysa L. Cole[1,2], John S. Gunn[1,2]

[1]The Ohio State University, Columbus, OH, USA. [2]Abigail Wexner Research Institute at Nationwide Children's Hospital, Columbus, OH, USA

Abstract

INTRODUCTION: *Salmonella enterica* serovar Typhi (*S.* Typhi) causes typhoid fever, a systemic illness in humans, in which 2-5% of patients become chronic carriers from biofilm formation on cholesterol gallstones. Typhoid fever lacks a direct *in vivo* model, as *S.* Typhi is host restricted to humans. We demonstrate that the immunocompetent collaborative cross mouse strain CC003/Unc can be used as a novel model of chronic typhoid fever to assess efficacy of novel therapeutic treatments and elucidate the role of the S. Typhi virulence factor Vi-antigen.

METHODS: Mice were fed a lithogenic diet (1% cholesterol and 0.5% cholic acid) for 6 weeks to induce gallstone formation and subsequently intraperitoneally infected with *S*. Typhi. At 21 days post infection (dpi), mice were euthanized; cardiac blood was collected; and the gallbladder, liver, and spleen were aseptically removed, homogenized, and plated for bacterial enumeration. Immunoglobulins against Vi-antigen were measured in serum using a direct ELISA.

RESULTS: We recovered *Salmonella* within all organs at 21 dpi, and the lithogenic diet contributed to higher bacterial burden in the gallbladder. Daily intraperitoneal administration of novel biofilm inhibitors combined with ciprofloxacin beginning at 10 dpi significantly decreased the amount of *S*. Typhi in the gallbladder. Competition experiments showed decreased relative fitness in each organ for Vi-antigen deficient S. Typhi, and Vi-antigen specific antibodies are produced in wild-type infection.

CONCLUSION/IMPACT: We determined that biofilm inhibitors are effective *in vivo* against *S.* Typhi and the CC003/Unc mice are a promising, physiologically relevant murine model of typhoid fever for future studies.

P22 *Staphylococcus aureus* Superantigens Suppress Sebaceous Gland Lipids to Promote Skin Colonization

Laine E. Feller[1], Zhiyang Li[1], Diane Hong[1], Toan Bui[1], Sabrina Kline[1], Meng-Jen Wu[1], Jing Zhang[1], Yu Wang[1], Shardulendra P. Sherchand[2], M. Javad Aman[2], Stephen W. Tuffs[3], Heidi H. Kong[4], Sima Rozati[1], Nathan K. Archer[1]

[1]Johns Hopkins School of Medicine, Baltimore, MD, USA. [2]AbVacc, Rockville, Maryland, USA. [3]University of Victoria, Victoria, British Columbia, Canada. [4]National Institutes of Health, Bethesda, Maryland, USA

Abstract

Staphylococcus aureus skin colonization exacerbates numerous inflammatory skin diseases, including atopic dermatitis (AD), Netherton syndrome and cutaneous T cell lymphoma (CTCL). Yet, how *S. aureus* surmounts the skin barrier to initiate pathogenic colonization is not fully understood. Using a preclinical model of AD-like skin inflammation induced by *S. aureus* epicutaneous exposure in C57BL/6J mice (females, 6-10 weeks), we discovered that *S. aureus* superantigen toxins (SAgs) promoted an 8-fold increase in skin colonization ($p<0.001$) in a mechanism involving reduced sebaceous gland numbers in the skin ($p<0.0001$). This was reinforced by RNAseq analysis, which revealed that SAgs suppressed sebocyte maturation and lipid synthesis genes (FDR<0.05). Similarly, lipidomics from skin scrapes uncovered that *S. aureus* SAgs reduced sebum-derived triglycerides, particularly those containing long-chain fatty acids with anti-staphylococcal activity ($p<0.05$). To translate our preclinical findings, we evaluated skin biopsies from healthy (n=15), AD (n=28), and CTCL (n=80) patients. Notably, we found that AD and CTCL patients had pronounced sebaceous gland abnormalities, including fewer mature sebaceous glands ($p<0.0001$), reduced lipid vacuolation ($p<0.05$), and smaller sebocytes ($p<0.0001$) compared to healthy controls. Moreover, when CTCL patients were stratified by their history of skin infection and infection type, *S. aureus* skin infection had the strongest effect on reduced sebocyte size ($p<0.0001$), reinforcing the relationship between *S. aureus* and sebaceous gland dysfunction. Collectively, these findings reveal how *S. aureus* interacts with sebaceous glands to overcome the skin barrier, with implications for therapeutics that restore skin homeostasis in inflammatory skin diseases with *S. aureus* involvement.

P23 Historical Microscopic Control Data of the Central and Peripheral Nervous System in Beagles

Samantha Hicks-Peña[1,2], *Charlotte Hollinger*[1], *Molly Liepnieks*[1], *Sarah Coe*[1]

[1]Inotiv, Kalamazoo, MI, USA. [2]Texas A&M University CVM, College Station, TX, USA

Abstract

Beagles are vital in drug development as a standard model for non-clinical safety toxicology studies. Establishing historical control data (HCD) aids in understanding animal models and helping to distinguish spontaneous background findings from procedural and/or drug-induced effects. The goal of this HCD review was to document the type and incidence of microscopic findings in the central and peripheral nervous system of control Beagles from recent general toxicology studies. 19 Beagle dog studies (oral gavage, intravenous injection, subcutaneous injection, and intra-articular injection) from 2022–2025 were included. Studies were 1 to 39 weeks and animals were single source with age 5 to 18 months. Microscopic data from 68 male and 67 female control animals was reviewed and findings from the brain, spinal cord, and sciatic nerve were collated. Findings included: minimal extramedullary hematopoiesis (EMH) in the choroid plexus of 2 males (1.5% incidence, 3% males); minimal focal gliosis in the brain of 1 male (0.7% incidence, 1.5% males); and minimal perivascular mononuclear cell infiltrates in the meninges of 1 female (0.7% incidence, 1.5% females). No findings were recorded in the spinal cord or sciatic nerve. Microscopic findings were rare in the central and peripheral nervous system of beagles and consistent with minor spontaneous background lesions. The most common finding (1.5% incidence) was minimal EMH in the choroid plexus. Maintaining up-to-date HCD aids in monitoring animal model health and distinguishing test-article-related effects from spontaneous findings in safety toxicology studies.

P24 Withdrawn

P25 Hepatotoxicity Associated with Portosystemic Shunts in C57BL/6J Mice Fed a High Fat Diet with Butylated Hydroxyanisole

Claire Kazen-Thompson, Rani S. Sellers, Summer Truong, Tigist Tamir

University of North Carolina, Chapel Hill, NC, USA

Abstract

Metabolic-associated steatotic liver disease (MASLD) is the most common chronic liver disease globally. The obesity-prone C57BL/6 mouse strain on a high fat diet (HFD) is used to model MASLD. Butylated hydroxyanisole (BHA), an antioxidant, can mitigate weight gain and insulin resistance in C57BL/6 fed a HFD. In a study using C57BL/6J mice fed HFD, HFD + BHA (HB), or control chow on a rotating schedule, four females consuming HB experienced unexpected weight loss; three were euthanized and necropsied and the fourth was found dead. Tissues were collected in 10% NBF, routinely processed, and H&E stained. IHC for cleaved caspase-3 (CC3) to identify apoptotic cells was performed on liver sections. Comparator livers from C57BL/6J mice from unrelated studies were similarly evaluated. All three HB mice had diffuse hepatocellular injury including vacuolar degeneration, cytokaryomegaly, multinucleation, cytoplasmic alteration, increased mitotic figures, and multifocal single-cell necrosis/apoptosis. Additionally, all three mice had findings consistent with porto-systemic shunt (PSS). CC3 IHC in HB livers compared to control comparators confirmed increased apoptosis. PSS, common in C57BL/6 mice, exacerbates lesions in MASLD models. The proposed mechanism of liver injury in HB mice is mitochondrial dysfunction. HFD, BHA, and PSS are associated with mitochondrial dysfunction, increased reactive oxygen species, and decreased ATP generation. While each condition alone may be clinically silent, combined they may limit ATP generation and overwhelm hepatocellular antioxidant capacity. The high prevalence of PSS in C57BL/6 mice should be considered when planning toxicity studies using this strain.

P26 A Novel Double *abcb4/abcg2a* Knockout Zebrafish Model for Studying ABC Transporter–Mediated Drug Efflux and Toxicity

Chaunte Lewis[1,2], Joanna Thomas[1], Blake Carrington[3], Kevin Bishop[3], Robert Robey[1]

[1]Laboratory of Cell Biology, Center for Cancer Research, National Cancer Institute, National Institutes of Health, Bethesda, MD, USA. [2]CBSTP,Center for Cancer Research, National Cancer Institute, National Institutes of Health, Bethesda, MD, USA. [3]Zebrafish Core, National Human Genome Research Institute, National Institutes of Health, Bethesda, MD, USA

Abstract

INTRODUCTION: ATP-binding cassette (ABC) transporters, principally ABCB1 and ABCG2, are multidrug efflux transporters that actively efflux drugs and toxic compounds against a concentration gradient. ABC transporters are located at barrier sites, such as epithelial cells lining the gastrointestinal tract where they limit oral drug bioavailability, and capillary endothelial cells at the blood-brain barrier where they prevent brain penetration of chemotherapy. While mouse models are often used to study the *in vivo* role of these transporters, their utility is limited for large-scale pharmacological studies. To overcome this challenge, we investigated the zebrafish as an *in vivo* model for the study of ABC transporters.

METHODS: Zebrafish homologs of human ABCB1 and ABCG2, abcb4 and abcg2a, share many substrates with their human counterparts. Knockout zebrafish lines (*abcb4*−/−, *abcg2*a−/−, and double knockout) were generated using CRISPR/Cas9. Five-day post-fertilization larvae were assessed for uptake of fluorescent substrates and sensitivity to toxic substrates.

RESULTS: *abcb4*−/− zebrafish exposed to rhodamine 123, and *abcg2a*−/− zebrafish exposed to Hoechst 33342, exhibited increased accumulation of fluorescent dye within intestinal cells along the gastrointestinal tract compared to wild-type zebrafish. Double knockout fish accumulated both substrates within intestinal cells compared to wild-type zebrafish. Additionally, *abcb4*−/−, *abcg2a*−/−, and double knockout larvae displayed decreased survival following exposure to toxic substrates compared with controls.

CONCLUSION: This study establishes an ABC transporter knockout zebrafish model, providing a scalable *in vivo* system to investigate substrate toxicity and mechanisms of multidrug resistance.

IMPACT: This platform may facilitate higher-throughput screening approaches and improve our understanding of ABC transporter contributions to pharmacology and toxicology.

P27 Recovery Mechanism of Drug-Induced Vacuolar Lesions of the Adrenal Cortex After Drug Withdrawal

Ryo D. Obara[1,2], Yuki Kato[1], Yoshiji Asaoka[1], Yukie Murata[1], Hiroyuki Oka[1], Takeshi Izawa[2], Mitsuru Kuwamura[2]

[1]Shionogi & Co., Ltd., Osaka, Japan. [2]Osaka Metropolitan University, Izumisano, Japan

Abstract

INTRODUCTION/OBJECTIVES: Drug-induced vacuolar lesions (lipidosis) in the adrenal cortex are occasionally observed in nonclinical toxicity studies; however, their reversibility is often difficult to interpret due to limited information on recovery time course and underlying mechanisms. In our internal drug development programs, we previously encountered adrenal cortical vacuolation for which assessment of recovery potential proved challenging. This study aimed to investigate the chronological recovery process of vacuolar lesions induced by the steroidogenesis-inhibiting compound aminoglutethimide in rats.

EXPERIMENTAL DESIGN/METHODS AND MATERIALS: Crl:CD(SD) rats received aminoglutethimide for 2 weeks, followed by recovery periods of 2, 4, and 12 weeks. The adrenal glands were examined histopathologically and immunohistochemically and BrdU pulse-chase analysis were also conducted to investigate the recovery process.

RESULTS: Adrenocortical vacuolar lesions were observed at the end of the dosing period. These lesions consisted of lipid-laden adrenocortical cells and aggregations of foamy macrophages scavenging dead cells with liberated lipids. Lesions persisted for up to 4 weeks of recovery and were almost completely resolved after 12 weeks, with minimal lesions remaining in the zona reticularis. During recovery, vacuolar lesions were first resolved in the upper zona fasciculata after 2 weeks. BrdU pulse-chase analysis suggested that newly generated adrenocortical cells originated in this area and migrated toward the zona fasciculata and zona reticularis.

CONCLUSIONS: Macrophage-mediated clearance of dead cells and liberated lipids with centripetal migration of newly generated adrenocortical cells appear to contribute to lesion recovery.

IMPACT STATEMENT: These findings provide useful information for evaluating the reversibility of compound-induced adrenocortical vacuolar lesions.

P28 Comparative Evaluation of Historical Control Hematology, Coagulation, and Clinical Chemistry Test Results between Sprague-Dawley and Wistar-Han Rats

Vasilis C. Pliasas, Charles E. Wiedmeyer

Charles River Laboratories, Mattawan, MI, USA

Abstract

Routine clinical pathology testing in rodent models remains a fundamental component of nonclinical pharmaceutical safety assessment. Although Sprague-Dawley rats have historically been the most commonly utilized strain in toxicology studies, the use of Wistar-Han rats has increased over the past two decades due to their greater longevity and utility in longer-term studies. Despite their extensive use, comparative data on standard clinical pathology parameters between these two rodent strains remain limited. The purpose of this study was to investigate and characterize differences of toxicological relevance between Sprague-Dawley and Wistar-Han rats by analyzing historical control clinical pathology data. Clinical pathology values from studies conducted at a single contract research organization facility from 2019 to 2024 were compiled, including 1,538 animals, stratified by strain, sex, and age. Data were then statistically analyzed to examine inter-strain differences. The most pronounced differences between the two rodent strains were observed in hematology parameters, particularly white blood cell, neutrophil, lymphocyte, and platelet concentrations, with Sprague-Dawley rats demonstrating significantly higher values compared to Wistar-Han rats. Several additional, albeit smaller, differences in clinical chemistry and coagulation parameters were also identified. These findings underscore the importance of considering the rodent strain used when interpreting clinical pathology data, as baseline variations may influence the assessment of study-related outcomes. Accordingly, the use of strain-specific historical control data is essential to ensure accurate data interpretation in nonclinical safety studies.

P29 Immunohistochemical Delineation of Macrophage Functional States for Disease Characterization

Dayananda Siddappa, Ingeborg M. Langohr, Catherine King, Tatyana Taksir, Cynthia Shapiro, Colleen Maloney, Agnes Cheong, Timothy Hammond, Caroline Morel, Dinesh S. Bangari

Sanofi, Cambridge, MA, USA

Abstract

Macrophages are innate immune cells of the mononuclear phagocytic system with diverse developmental origins and marker expression profiles reflecting their functional state. They perform critical functions including phagocytosis, inflammation regulation, cytokine production, and tissue remodeling. The functional status of tissue macrophages has been associated with various diseases including autoimmune disorders, neurodegenerative diseases, cardiovascular disease, and cancer. Upregulation of macrophage markers — IBA1, CD68, and GPNMB — has been reported in mouse models of inflammatory and degenerative diseases. Using immunohistochemistry (IHC), we systematically characterized the expression patterns of these markers across multiple mouse models of human disease to establish a framework for macrophage-based disease characterization.

In the 5XFAD-hTREM2 KI Alzheimer's disease model, brains showed an increased level of IBA1$^+$, CD68$^+$, and GPNMB$^+$ area compared to wild type (WT) mice, with CD68 and GPNMB labeling activated macrophages compared to the broadly expressed pan-macrophage marker IBA1. In the Fra2 transgenic model of Type 2 pulmonary inflammation, GPNMB$^+$ macrophages were markedly increased in the alveoli relative to WT mice. Transgenic mouse models of lysosomal storage disease showed increased GPNMB$^+$ macrophages in liver tissue and elevated IBA1$^+$ and GPNMB$^+$ microglia in brain tissue. Notably, GPNMB$^+$ cells were exclusively localized to diseased tissue areas across all transgenic mouse models, confirming GPNMB as a disease-associated activation marker.

We propose a three-marker IHC panel — IBA1 for macrophage census, CD68 for phagolysosomal activation, and GPNMB for disease-associated reactive macrophages — to distinguish macrophage presence from functional activation states. This framework provides a robust histopathological tool for disease characterization, monitoring, and therapeutic screening.

P30 Azoxymethane-Treated Pirc Rats as an Accelerated Model of Colorectal Cancer

Allison C. Boone[1,2], Ricardo Cortes[1,2], Xuying Zhang[3,2], Krishna Latha Kanchi[2], Willie Cunningham[2], Peter Pediaditakis[1,2], Thai-Vu Ton[2], Arun Pandiri[2]

[1]Experimental Pathology Laboratories, Inc., Morrisville, NC, USA. [2]Comparative and Molecular Pathogenesis Branch, Division of Translational Toxicology, National Institute of Environmental Health Sciences, Research Triangle Park, NC, USA. [3]Gap Solutions, Herndon, VA, USA

Abstract

INTRODUCTION: Tumor latency in F344 rats treated with azoxymethane (AOM) is approximately 30 weeks, highlighting the need for an accelerated animal model of colorectal cancer (CRC).

EXPERIMENTAL DESIGN: We hypothesized that combining genetic susceptibility in the Polyposis-in-Rat-Colon (Pirc; F344/NTac-Apc^{am1137}) rat with AOM exposure would accelerate colon tumor development and reduce latency, establishing a faster model of CRC.

METHODS AND MATERIALS: Male and female Pirc rats, 8-12 weeks old, and wildtype (WT) F344 littermates (n=10/group) received AOM (15 mg/kg, SC) on study days 1 and 8. Body weights were recorded weekly, colonoscopies were performed monthly, and tumors were assessed grossly and microscopically at 6 months.

RESULTS: At 4 weeks post-exposure, colonoscopy showed an approximately 2-fold greater tumor burden in AOM-treated Pirc males and females relative to corresponding Pirc controls. Clinical signs were observed by 3 months post-exposure in Pirc males and females, indicating a 3-month reduction in tumor latency. At necropsy, AOM significantly increased tumor multiplicity in Pirc males (42.9±14.2, $p=7.19\times10^{-5}$) and females (19.3±12.6, $p=9.6\times10^{-4}$), whereas the effect was modest in WT males (0.44±0.73, p=0.062) and absent in WT females. Colon weights were also significantly increased in AOM-treated Pirc males (p=0.003) and females (p=0.00094) compared with corresponding controls.

CONCLUSION: These findings support a synergistic effect of genetic susceptibility conferred by the Pirc background and AOM exposure on colon tumor development, establishing this as an accelerated rat model of CRC.

IMPACT STATEMENT: The exacerbated tumor development in AOM-treated Pirc rats supports its utility for investigating CRC biology and evaluating therapeutic strategies.

P31 Brain Pathology in Irradiated Nonhuman Primates: Vascular Injury is Radiation Dose Dependent

Clemer Abad[1], John Olson[1], George Schaaf[2], J. Mark Cline[1]

[1]Department of Pathology, Section of Comparative Medicine, Wake Forest University School of Medicine, Winston Salem, NC, USA. [2]Department of Radiation Oncology, Wake Forest University School of Medicine, Winston Salem, NC, USA

Abstract

INTRODUCTION: Survivors of total-body irradiation (TBI) can develop comorbidities years after exposure, including vascular injury that primarily affects white matter across different brain regions.

EXPERIMENTAL DESIGN: This retrospective study evaluated 153 rhesus macaques that died between 2008 and 2026. The cohort included 32 non-irradiated controls and 121 animals exposed to acute TBI (2.0 to 10.0 Gy; 1-17 years post-exposure). Animals were grouped by irradiation status (yes/no) to assess long-term brain lesions.

METHODS: Clinical records and pathology reports were used to assess brain lesions, including focal hemorrhages, focal necrosis, focal inflammation, and focal hemosiderosis. Statistical tests used were Wilcoxon/Kruskal-Wallis, Fisher's exact, and Logistic regression.

RESULTS: A total of 18 irradiated animals had focal hemorrhages, while zero non-irradiated ($p<0.01$). Age at death was lower in irradiated (11.76 ± 4.17) compared to non-irradiated (17.71 ± 4.23, $p<0.01$). Irradiated animals had more focal hemorrhages than non-irradiated (15% vs 0%, $p<0.01$). Focal hemorrhages increased with radiation dose ($p<0.001$), whereas hemosiderosis increased with age ($p<0.0068$). No other lesions were associated with radiation exposure.

CONCLUSIONS: Long-term survivors of acute TBI exhibit delayed brain lesions, predominantly focal hemorrhages.

IMPACT STATEMENT: These findings highlight that radiation-related vascular injury is present after irradiation exposure. This work may contribute to future risk-mitigation strategies for cancer survivors and individuals exposed to radiation in occupational or accidental settings.

P32 Comparative Pathology of a Macaque Model of Bardet-Biedl Syndrome due to BBS7 Mutation

Nathan P. Crilly, Brian Lamendola, Anne Lewis, Kathy Grant

Oregon Health and Science University, Beaverton, OR, USA.

Abstract

Bardet-Biedl Syndrome (BBS) is a rare progressive genetic disorder characterized by retinal photoreceptor degeneration, renal disease, obesity, polydactyly, and orodental abnormalities. Most clinical features are absent at birth but become more severe over the first two decades of life, with retinopathy generally being the first symptom, while renal failure is the major cause of mortality. BBS is a ciliopathy, driven by dysfunction of proteins in the BBSome complex which controls ciliary protein trafficking.

Recently, a naturally occurring frameshift mutation in the BBS7 gene has been identified in rhesus macaques at the Oregon National Primate Research Center, which recapitulates features of the human BBS phenotype. This nonhuman primate (NHP) model has been used to explore disease progression and test new therapeutics. Here, we describe the gross and histopathological features of the NHP BBS model and compare them to human pathologies. As in humans, the major features of the NHP model include retinal and renal degeneration. Juvenile NHPs exhibit progressive retinal atrophy. Affected animals also exhibit progressive renal failure, exhibiting increasing fibrosis and interstitial nephritis. Increased adiposity is also noted. Although the major diagnostic features of BBS are recapitulated in the NHP model, several of the minor features are absent or inconsistently observed, including craniofacial abnormalities and polydactyly. However, given the heterogeneity of human pathology, this is not entirely unexpected.

The BBS NHP model demonstrates the importance of collaboration between animal care workers, pathologists, geneticists, and scientists to identify, characterize, and utilize naturally occurring animal models to improve our understanding of human disease.

P33 Assessment of Orchidometric Testicular Volume as a Tool for Selecting Sexually Mature Male Rhesus Monkeys for Nonclinical Toxicology Studies

Maria C. Cuitino, Takayuki Tsuchiya, Sabu Kuruvilla

Nonclinical Drug Safety, Merck & Co., Inc., Rahway, NJ, USA

Abstract

INTRODUCTION: Accurate identification of sexually mature male nonhuman primates is critical for nonclinical toxicology studies requiring mature animals. Common indicators of sexual maturity such as age and body weight are unreliable, and semen evaluation is impractical for general toxicology studies. Orchidometric testicular volume has been shown to predict sexual maturity in cynomolgus monkeys, but its utility in rhesus monkeys is not well characterized.

OBJECTIVE: This study evaluated orchidometric testicular volume as a practical indicator of sexual maturity in male rhesus monkeys.

EXPERIMENTAL DESIGN/METHODS: In-life testicular volume was measured using an orchidometer in 85 control male rhesus monkeys (*Macaca mulatta*) from 29 nonclinical toxicology studies (age range 1.6–6.7 years) on the day of necropsy. Terminal body weight and testis weight (including epididymis) were also recorded. Sexual maturity status/score was assigned based on histomorphologic evaluation of the testis, epididymis, and prostate using established criteria. Associations between testicular volume, histologic maturation score, testis weight, age, and body weight were assessed.

RESULTS: Testicular volume showed a positive association with both histologic maturity status/score and testis weight across maturation stages. Age and body weight were less consistently associated with histologic maturity status, particularly around the peripubertal period.

CONCLUSION: These preliminary results suggest that orchidometric testicular volume may be a practical and reliable tool for identification of sexually mature male rhesus monkeys prior to study initiation.

IMPACT STATEMENT: This approach could streamline animal selection and increase confidence in identification of sexually mature rhesus monkeys for nonclinical toxicology studies.

P34 INHAND: International Harmonization of Nomenclature and Diagnostic Criteria for Lesions—An Update

Emily Meseck[1], Ute Bach[2], Alys Bradley[3], Mark Cesta[4], Stacey Fossey[5], Shim-mo Hayashi[6], Matt Jacobsen[7], Rupert Kellner[8], Victoria Laast[9], Thomas Nolte[10], Kumiko Ogawa[11], Susanne Rittinghausen[12], Junko Sato[13], John Vahle[14], Katsuhiko Yoshizawa[15]

[1]Preclinical Safety, Novartis Biomedical Research, East Hanover, NJ, USA. [2]Pathology & Clinical Pathology, Bayer Aktiengesellschaft, Wuppertal, Germany. [3]Elphinstone Research Center, Charles River Laboratories Edinburgh Ltd, Tranent, Scotland, United Kingdom. [4]Division of Translational Toxicology, National Institute of Environmental Health Sciences, Research Triangle Park, NC, USA. [5]Preclinical Safety, AbbVie Inc, North Chicago, IL, USA. [6]National Institute of Heal Sciences, Osaka, Japan. [7]Clinical Pharmacology & Safety Sciences, AstraZeneca, Cambridge, United Kingdom. [8]Chemical Safety & Toxicology, Fraunhofer Institute for Toxicology & Experimental Medicine ITEM, Hannover, Germany. [9]Labcorp, Madison, WI, USA. [10]Global CPS Mental & Eye Health & EA, Boehringer Ingelheim Pharma GmbH & Co. KG, Biberach, Germany. [11]Toxicology, Hoshi University, Tokyo, Japan. [12]Department of Pathology & Clinical Pathology, Fraunhofer Institute for Toxicology & Experimental Medicine ITEM, Hannover, Germany. [13]Mediford, Tokyo, Japan. [14]Toxicology & Pathology, Lilly Research Laboratories, Indianapolis, IN, USA. [15]Department of Innovative Food Sciences, Mukogawa Women's University, Hyogo, Japan

Abstract

Since the inception of INHAND (International Harmonization of Nomenclature and Diagnostic Criteria for Lesions in Rats and Mice) in 2005, a Global Editorial Steering Committee (GESC) composed of representatives from the Japan, Europe, British and US Societies of Toxicologic Pathology has coordinated objectives and publications of the ongoing project. Development of terminology for rodent organ systems and non-rodent species is the responsibility of working groups, with globally recognized experts from North America, the United Kingdom, Europe, Japan and other regions.

All rodent organ systems have been published in *Toxicologic Pathology* or the *Journal of Toxicologic Pathology*, including Respiratory, Hepatobiliary, Urinary, Nervous, Male and Female Reproductive, Mammary, Zymbal, Clitoral and Preputial Glands, Hematolymphoid, Integument and Soft Tissue, Digestive, Cardiovascular, Skeletal, Special Senses and Endocrine Systems. Publications are available as journal supplements and on www.goReni.org, where change control updates are uniquely available. Rabbit, Non-human Primate, Mini-pig and Dog terminology was published in 2021. Non-rodent ocular toxicity nomenclature was published in *Toxicologic Pathology* in 2024 and the final non-rodent species, Fish, was published in *Journal of Toxicologic Pathology* in 2026. The Medical Device working group is making progress as well.

INHAND offers nomenclature, diagnostic criteria, differential diagnoses, images, commentary and references to guide recording of microscopic findings in nonclinical toxicity and carcinogenicity studies. INHAND GESC representatives work with Clinical Data Interchange Standards Consortium (CDISC) to incorporate INHAND terminology as preferred terminology for SEND (Standard for Exchange of Nonclinical Data) submissions to the US FDA, with wide acceptance of this nomenclature by global health authorities.

P35 Comparison of Background Histologic Findings in Cynomolgus Macaques of Philippine vs. Other Asian Origin

Melissa Graham[1], Kelly Ashcroft-Hawley[2], Lars Mecklenburg[3], Julie Turner[1], Jim Saul[2], Victoria Laast[1], Alok Sharma[1]

[1]Labcorp, Madison, WI, USA. [2]Labcorp, Harrogate, United Kingdom. [3]Labcorp, Muenster, Germany

Abstract

Comparison of spontaneous histopathologic findings between macaques of Mauritian, Chinese, Vietnamese, and Cambodian origin previously revealed minor variations not impacting suitability for toxicology studies (Chamanza et al, 2022). With research animal supply chain changes, institutions may acquire macaques from different sources, including the Philippines. We compare histologic findings in control Philippine vs. Cambodian, Chinese, and Mauritian cynomolgus macaques.

Labcorp Madison's historical control database was searched for histologic findings in control animals from 7 randomly selected studies for each origin (Cambodian, Chinese, Mauritian, and Philippine). Incidence rates were compared using Fisher's exact tests.

Findings were similar in Philippine vs. other origin macaques with most variations relating to mononuclear cell infiltrates. Philippine macaques exhibited decreased incidence of mononuclear cell infiltrates in females in the brain, cecum, esophagus, mandibular salivary gland, pancreas, and kidney, and in males in the prostate, skin/subcutis, eye, and stomach. Other findings with decreased incidence were thyroid cysts (males), ectopic thymus in thyroid (females), thymic cysts (females), protozoal parasites in colon (both sexes) and cecum (females), increased fibrous connective tissue in testis, and mineralization in ovary. Philippine macaques showed increased incidence of perivascular mononuclear cell infiltrates in brain (males) and mononuclear cell infiltrates in adrenal cortex (both sexes).

Control Philippine macaques display histologic findings similar in incidence to Cambodian, Chinese, and Mauritian macaques, with most variability related to mononuclear cell infiltrates.

These findings support the suitability of Philippine macaques for toxicology studies when background differences are appropriately considered.

P36 Reference Intervals for Clinical Pathology Parameters in Sprague-Dawley Rats in Juvenile Animal Toxicity Studies

Aradhana Gupta[1], Stavros Zinonos[2], Lindsay Tomlinson[3], Taylor Hulten[4], Stephanie S. Powlin[5], Nicola Powles Glover[6], Keith R. Shockley[7], Alan M. Hoberman[8], Zhiyong Xie[9], Stephanie L. Rayhon[10], Tacey White[11], Shermaine Mitchell-Ryan[12], Connie L. Chen[12]

[1]Boehringer Ingelheim Pharmaceuticals, Inc, Ridgefield, CT, USA. [2]Pfizer, Pearl River, NY, USA. [3]Alnylam Pharmaceuticals, Cambridge, MA, USA. [4]Pfizer, Groton, CT, USA. [5]Takeda Pharmaceutical International Co, Cambridge, MA, USA. [6]ExxonMobil, Houston, TX, USA. [7]National Institute of Environmental Health Sciences, Research Triangle Park, NC, USA. [8]Charles River Laboratories, Inc., Horsham, PA, USA. [9]Fosun Pharma, Shenzhen, China. [10]Johnson & Johnson, Spring House, PA, USA. [11]Tacey White Toxicology Consulting, LLC, Glenside, PA, USA. [12]Health and Environmental Sciences Institute, Washington, DC, USA

Abstract

Juvenile animal toxicology studies in rats are often important for evaluating age-related clinical pathology changes relevant to pediatric safety assessment but interpretation may be hindered by limited historical control data. Therefore, we sought to establish comprehensive age- and sex-specific reference intervals for hematology, clinical chemistry, and coagulation parameters in juvenile Sprague-Dawley rats to enhance the evaluation of toxicologic pathology endpoints. Clinical pathology data was collected from control Sprague Dawley rats from juvenile toxicology studies conducted between 2007 and 2023 across six contract research organizations, and standardized statistical methods were applied for outlier detection, normality assessment, and generation of reference intervals with 90% confidence limits across five developmental age categories (<4, 4–6, 6–8, 8–16, and >16 weeks) stratified by sex. Juvenile animals exhibited trends compared with adults, including lower red blood cell count, hemoglobin, hematocrit, mean corpuscular hemoglobin concentration, lymphocytes, total white blood cells, total protein, albumin, and creatinine that generally increased with age, whereas reticulocytes, mean corpuscular volume, red cell distribution width, phosphorus, alkaline phosphatase, cholesterol, and triglycerides were higher in younger animals and decreased with maturation; glucose, chloride, urea nitrogen, and total bilirubin had minimal age-related variation. These novel reference intervals in juvenile animals fill an important gap in providing a quantitative framework for distinguishing normal developmental variation from test article-related effects, and support more informed evaluation of clinical pathology findings in juvenile toxicology studies conducted within the field of toxicologic pathology.

P37 Regional Differences in Tissue Responses After Stent Deployment in Subclavian and Carotid Arteries in Swine Model

Atsushi Isobe, Ryan Callahan

TERUMO Neuro, Aliso Viejo, CA, USA

Abstract

INTRODUCTION: Carotid artery stenting is commonly used as a therapy for atherothrombotic stroke led by carotid artery stenosis. Preclinical studies primarily utilize carotid and subclavian arteries in swine as a target location. However, differences in post-stenting tissue responsesin the subclavian versus carotid arteries remain unclear.

EXPERIMENTAL DESIGN: Stents were implanted in carotid and subclavian arteries in the identical swine at a defined stent-to-artery ratio. Animals (n=6 per group) survived for 3 or 28 days, and samples were fixed, processed and stained with HE and Movat.

METHODS: Every section assessed injury, inflammation, fibrin, adventitial inflammation, luminal thrombus, endothelialization, neointimal maturity, media compressive hypocellularity, adventitial fibrosis and hemorrhage. Injury was scored on a 0-3 scale, others on 0-4. %stenosis was calculated by histomorphometry. Paired t-tests were applied.

RESULTS: Stent-to-artery ratio was comparable (subclavian vs. carotid = 1.19 ± 0.15 vs. 1.20 ± 0.09, p=0.84). At 28 days, subclavian artery had higher fibrin and hemorrhage scores (, respectively), and greater stenosis than carotid (subclavian vs. carotid, 1.61 ± 0.78 vs. 0.03 ± 0.17, p<0.05 for fibrin, 1.44 ± 1.04 vs. 0.03 ± 0.17, p<0.05 for hemorrhage, 27.26 ± 17.84 % vs. 15.20 ± 5.09 %, p<0.05 for stenosis), whereas other scores were similar at 3 and 28 days.

CONCLUSION: Neointimal healing was slower in subclavian than carotid arteries at 28 days. The mechanical motion from forelimb movement may cause tissue damage such as hemorrhage and fibrin, promoting neointimal growth.

IMPACT STATEMENT: These results may help preclinical researchers and companies more accurately interpret tissue reactions not only to stent material and deployment but also to anatomical motion.

P38 Withdrawn

P39 Dose-Dependent Early Fibrotic Remodeling in a Recurrent LPS-Induced Acute Lung Injury Rat Model: Translational Implications for Human ALI

Predrag Novakovic, Bo In Choi, Alexander-Yap Sia, Joseph Younan, William Lee, Kevin McInally

ITR Laboratories, Baie D'Urfe, Quebec, Canada

Abstract

BACKGROUND: Recurrent acute lung injury (ALI) is an increasingly recognized precursor to progressive pulmonary fibrosis. Preclinical models that characterize early fibrotic remodeling using standardized histopathologic criteria are essential for translational interpretation. This study evaluated dose-dependent fibrosis, lesion distribution, and associated respiratory function changes in a recurrent intratracheal (IT) lipopolysaccharide (LPS)-induced ALI rat model.

METHODS: Rats (n=6/group) received IT saline or LPS twice weekly (Days 1, 5, 10, 14) at 50 µg, 250 µg, or 500 µg (Days 1, 5, 10) and 400 µg (Day 14). Respiratory parameters were measured 4 h post-dose (Days 5 and 14) and prior to necropsy (Day 15). Lungs were examined histologically using INHAND terminology. Chronic/proliferative lesions were graded semi-quantitatively. Fibrosis was scored using Ashcroft and Modified scales, with Masson's trichrome as supportive evidence.

RESULTS: Fibrosis was dose-dependent in severity and distribution. Controls showed no fibrosis (mean Ashcroft=0). Rats receiving 50 or 250 µg LPS had minimal, multifocal interstitial fibrosis (mean Ashcroft=0.5) with mild septal thickening and persistent inflammation. The 500/400 µg group developed moderate, multifocal-to-coalescing fibrosis (mean Ashcroft=2.3; Modified=2.7) with septal expansion, increased collagen deposition, and broader lobar involvement. Concordance between scoring systems was strong, with slightly higher grades assigned by the Modified scale at moderate severity. Animals with greater fibrosis showed trends toward reduced minute volume and respiratory rate, without a clear correlation between fibrosis severity and function.

CONCLUSIONS: Recurrent IT LPS exposure produced reproducible, dose-dependent early fibrotic remodeling with limited functional impairment, supporting the model's translational relevance for recurrent human ALI.

P40 Background Thymic Epithelial Hyperplasia and Thymoma in rasH2 Transgenic Mice from 26-Week Carcinogenicity Studies

Sasmita Mishra[1], Vimala Vemireddi[2], Marcia Pereira Bacare[3], Molly Boyle[3], Mark Mense[3], Alok Sharma[2]

[1]Labcorp, Greenfield, IN, USA. [2]Labcorp, Madison, WI, USA. [3]Labcorp, Chantilly, VA, USA.

Abstract

INTRODUCTION: Since the FDA's approval in 2003, transgenic rasH2 (Tg.rasH2) mice have been used as alternative models to assess the carcinogenic potential of new drug candidates. While several published articles document spontaneous non-neoplastic and neoplastic findings in Tg.rasH2 mice, the incidence and morphologic criteria of proliferative thymic epithelial lesions have not been discussed in detail. Here we report the incidence and diagnostic morphologic criteria of non-neoplastic (epithelial hyperplasia) and neoplastic (benign and malignant thymoma) proliferative findings in the thymus.

METHODS: Historical control data from sixty-three 26-week rasH2 mouse studies were analyzed from 2012–2017 and 2018–2024 conducted at Labcorp, Madison, WI, to compare and to determine incidence trends over time and also the combined incidence from both intervals.

RESULTS: Compared with published literature, an increased incidence of epithelial hyperplasia was noted in both sexes, with a higher incidence in females (7.4%) versus males (3.4%). Benign thymomas occurred at a higher-than-published incidence in both sexes, with higher frequency in females (1.8%) vs. males (0.7%). Our data further documented the first occurrences of malignant thymoma in this mouse strain, which was also more common in females (1%) vs. males (0.7%). The epithelial features of selected proliferative findings were confirmed by immunohistochemistry (pan-cytokeratin).

CONCLUSION: Robust historical control data for thymic proliferative lesions in Tg.rasH2 mice can aid greatly in data contextualization and overall interpretation, especially when the tumor incidence in study control animals is unexpectedly high or low.

P41 Renal Tubular Injury in Naturally Occurring Arsenic Toxicosis in Cattle with Suspected Waterborne Exposure

Nikhil Sanjay Rao[1], Jenna Stockler[2], Rachel Neto[1]

[1]Department of Pathobiology, College of Veterinary Medicine, Auburn University, Auburn, AL, USA. [2]Department of Clinical Sciences, College of Veterinary Medicine, Auburn University, Auburn, AL, USA

Abstract

Arsenic toxicosis is an uncommon but significant cause of acute mortality in cattle, typically linked to environmental contamination. This report describes clinicopathologic, gross, and histopathologic findings in two cows from the same property with confirmed arsenic exposure and no identifiable point source. Both animals had nonspecific clinical signs, including lethargy, ataxia, diarrhea, and pigmenturia ("coffee-colored"). One cow died on the property and was submitted for necropsy, while the second was hospitalized shortly thereafter with worsening azotemia (BUN 89.4→113 mg/dL [R.I.: 7–17], creatinine 10.8→11.1 mg/dL [R.I.: 1–3]), prompting euthanasia. Despite investigation, no direct access to arsenic-containing products was reported; however, both animals had access to a nearby creek, representing the most proximal source of exposure. At necropsy, both cows had diffusely pale kidneys with bulging parenchyma; one also exhibited generalized edema and tricavitary effusions. Only one cow had modest ruminal hemorrhage and edema, abomasal microulcers, and intestinal petechiation. Both animals had consistent and severe renal lesions, characterized by subacute tubular epithelial degeneration, necrosis, and regeneration with tubular dilation, abundant granular to cellular casts, and marked interstitial edema. Toxicologic analysis confirmed elevated renal arsenic concentrations (8.3 ppm and 5.0 ppm, respectively; [toxic level > 3ppm wet weight]). These cases highlight the kidney as the most severely affected organ in subacute arsenic toxicosis and show the importance of environmental investigation to prevent additional exposures.

P42 Impact of Duration and Setting of Urine Collection on Urinalysis and Urine Chemistry Parameters in Non-Human Primates

Tiffany N. Scott[1], Frederic Morel[2], Gabriella Diamantino[1], Liza Bau-Gaudreault[1], Florence Poitout[1]

[1]Charles River Laboratories, Senneville, QC, Canada. [2]Charles River Laboratories, Sherbrooke, QC, Canada

Abstract

INTRODUCTION/OBJECTIVES: Urine collection from non-human primates (NHPs) involved in nonclinical studies is limited by food and water consumption and caging. While optimal urine quality is necessary for analysis, poor urine quality jeopardizes studies. The goal of this investigation was to compare urine data collected in different study settings.

METHODS/DESIGN: Three types of urine collection systems for NHPs were evaluated. NHPs were placed in metabolic cages overnight and urine was collected overnight (OC) or in the morning over 2 hours maximum (MSC). For MSC, clean cage pans were placed in the morning while lights were off, and urine was collected after turning the room lights on. Thirdly, NHPs were placed in metabolic cages only in the morning and urine was collected over 2 hours (MMC). Water and food access were not limited.

RESULTS: Differences were observed in urine volumes (1-130 mL for OC, 1-60 mL for MSC and MMC). Morning collections (MSC, MMC) limited food contamination, but higher urine specific gravity (USG) was noted when animals were placed in metabolic cages the night before (USG = 1.015-1.024 for MSC, vs 1.007-1.014 for OC). USG was low when animals were moved in the morning (MMC; 1.002-1.005). OC and MSC led to similar urine chemistry results, while MMC led to lower concentrations. Analyte normalization over creatinine led to better consistency between all collection methods.

CONCLUSION/IMPACT STATEMENT: Overnight separation of NHPs combined with morning short-term urine collection (MSC) is optimal for group-housed animals. Animals can be fed and should not be water deprived.

P43 Phenotypic Characterization of Fra-2 Transgenic Mice as a Model of Scleroderma

Yinglin Gao[1], Traci Wilgus[1], Luis Cheng[1], Bharathi Sundaram[1], Ted Kaplan[1], Abigail Gagliardi[2], Susannah Brydges[2], Lori Morton[1], Jon Popke[3], Prachi Sharma[3]

[1]Therapeutic Focus Areas, Regeneron Pharmaceuticals, Tarrytown, NY, USA. [2]Velocigene, Regeneron Pharmaceuticals, Tarrytown, NY, USA. [3]Drug Safety and Pharmacometrics, Regeneron Pharmaceuticals, Tarrytown, NY, USA

Abstract

BACKGROUND: Though Scleroderma–Interstitial Lung Disease (SSc-ILD) and Scleroderma–Pulmonary Hypertension (SSc-PH) drive mortality in systemic sclerosis, preclinical models underrepresent vasculopathy. Fra-2 (FOSL2) transgenic (Tg) mice spontaneously develop inflammation, vasculopathy, and tissue fibrosis, recapitulating key features of human SSc. Here, we evaluated skin and lung lesions in Fra-2 mice of 25 weeks age.

METHODS: FFPE lung and dorsal skin sections from H2kb prm–Fra-2 Tg and WT male mice (24–25 weeks age) were examined by H&E, Masson's trichrome, and SMA IHC and lesions analyzed.

RESULTS: Pulmonary hypertension in Fra2 Tg mice was confirmed with elevated right ventricular systolic pressure. Their lungs exhibited vasculopathy (intimal and medial proliferation, adventitial involvement, partial to near-complete luminal occlusion, rare intimal inflammatory infiltrates). Increased alveolar macrophages with eosinophilic crystalline material, rare interstitial neutrophils with few lymphocytes, and occasional perivascular mononuclear infiltrates also seen. Occasionally, these formed peripheral foci of consolidation. Masson's Trichrome staining demonstrated increased perivascular collagen, indicating moderate fibrotic remodeling. In skin, Fra-2 Tg mice had significantly increased minimal-to-mild neutrophilic and histiocytic dermal infiltrates and reduced subcutaneous adipose tissue, without changes in vascular density or dermal fibrosis. WT mice showed no significant lesions.

CONCLUSIONS: Fra-2 Tg mice develop pulmonary arterial remodeling with moderate fibrotic change and skin lipoatrophy with mild dermal infiltrates in absence of overt dermal fibrosis at 25 weeks of age.

IMPACT: Findings 1) support translational relevance of Fra-2 model for SSc-associated PAH and suggest vasculopathy may precede cutaneous fibrosis at 25 weeks age; 2) inform selection of timing and histologic endpoints for therapeutic studies.

P44 Toxicological Profile of Therapeutic Radionuclides and Radiopharmaceuticals in Animal Studies: A Scoping Review

Jong Il Shin, Jin Young Baik, Yiseul Choi, Eun Sang Lee, Yong Jin Lee, Kwang Il Kim

Korea Radioisotope Center for Pharmaceuticals, Korea Institute of Radiological and Medical Sciences (KIRAMS), Seoul, Republic of Korea

Abstract

Therapeutic radiopharmaceuticals enable targeted radiation delivery, but nonclinical safety reporting is heterogeneous. We conducted a scoping review to map study characteristics and analyze how clinical pathology and histopathology are assessed and reported in nonclinical studies.

PubMed was searched for rodent studies of therapeutic radiopharmaceuticals reporting at least one clinical pathology and/or histopathology endpoint. Charted data were summarized descriptively using narrative synthesis, tabulation, and visualization.

From 804 records, 75 studies were included. The most commonly used isotopes were ^{177}Lu, ^{211}At, ^{225}Ac, and ^{212}Pb. Mouse models predominated, and 62.3% of studies used separate toxicity cohorts. Clinical pathology was reported in 68 studies, histopathology in 51 studies, and 29 studies reported all endpoints. Frequently reported parameters included WBC (n=50), BUN (n=39), and creatinine (n=34). Kidney was the most frequently examined for histopathology (n=41) and the organ most commonly affected by lesions (n=21). Maximum follow-up ranged from 4 days to 52 weeks, with no apparent trend with radionuclide physical half-life. Common findings included decreases in WBC (n=34) and PLT (n=28), and elevations in BUN (n=16) and creatinine (n=11), with renal lesions including tubular karyomegaly, glomerulosclerosis, tubular dilatation, and interstitial fibrosis. Median intolerable activity levels were 27.75 MBq (^{177}Lu), 37.00 kBq (^{225}Ac), 1.42 MBq (^{211}At), and 740.00 kBq (^{212}Pb). However, several radionuclides lacked identifiable intolerable levels.

Nonclinical radiopharmaceutical toxicology shows substantial heterogeneity, but hematologic suppression and renal injury were repeatedly observed. More consistent reporting of endpoints, pathology panels, and observation periods may improve interpretability of nonclinical safety evaluation across radionuclides, vector platform, and experimental designs.

P45 Procedure-Related Findings Associated with Subcutaneous Injection in Non-Human Primates Utilized in Preclinical Toxicity Studies

Nick Vetter, Keith Nelson

Inotiv, Kalamazoo, MI, USA

Abstract

Recognition and differentiation of procedure-related findings versus test-article effects at the injection site is a critical component of determining potential toxicity in preclinical subcutaneous injection studies. Description of background injection site findings in non-human primates (NHPs) is limited in recent literature. A retrospective review of historical control data was conducted to identify and describe procedural findings observed with subcutaneous injections in NHPs. Compiled microscopic data included 104 injection sites from 44 control Cynomolgus macaques (*Macaca fascicularis*) in six toxicology studies over four years (2022–2025). Study main phase duration was 28 to 275 days, with time since final dosing of 1-36 days. Sites were categorized as acute (1 day since final dose) or subacute/chronic (≥ 7 days since final dose). Terminology was aligned across studies. Common findings (≥ 20% incidence) included fibroplasia (acute and subacute/chronic) and hemorrhage, mixed cell infiltration/inflammation, and macrophage infiltration/inflammation (acute). Infrequent findings (10–20%) comprised eosinophilic extracellular material (acute) and mixed cell infiltration/inflammation, hemorrhage, macrophage infiltration/inflammation, mononuclear cell infiltration, and muscle degeneration/necrosis (subacute/chronic). Rare findings (< 10%) included pseudocyst, follicular atrophy, muscle degeneration/necrosis, mononuclear cell infiltration, macrophage pigment accumulation, and congestion (acute) and neutrophil infiltration, crust, hyperkeratosis, and granuloma (subacute/chronic). Subcutaneous injection site findings in control NHPs may reflect a mixture of mechanical trauma (injection volume, needle, etc), vehicle formulation, and associated inflammatory/healing responses that can confound interpretation of TA-related findings and toxicity at the injection site. Understanding and consideration of these confounding factors allows more accurate assessment of localized TA-related effects.

P46 Application of an Artificial Intelligence Model for Quantitative Evaluation of Rat Bone Marrow Cell Lineages in Toxicology Studies

Mehrdad Ameri[1], Deon Hildebrand[2], Peter Clements[2]

[1]GlaxoSmithKline, Collegeville, PA, USA. [2]GlaxoSmithKline, Stevenage, Hertfordshire, United Kingdom

Abstract

INTRODUCTION: Bone marrow (BM) evaluation is a key component of nonclinical toxicology studies for identifying treatment-related hematopoietic effects. Conventional assessment relies on semiquantitative microscopic interpretation by pathologists, with lineage shifts inferred from morphology in H&E-stained sections. This approach can be time-intensive and subject to inter-observer variability, particularly when estimating subtle changes in cellularity or lineage distribution. Advances in artificial intelligence (AI) offer the potential to provide objective, reproducible, and quantitative assessments of BM composition. This study describes the development and application of an AI model for automated detection and enumeration of BM cell lineages in H&E-stained rat sections.

METHODS: Whole-slide images of H&E-stained rat femur and sternum sections from 24 historical control animals were used to train a dense convolutional neutral network (CNN). Veterinary pathologists annotated representative cells from BM hematopoietic lineages, including myeloid, erythroid, megakaryocytic, lymphoid and macrophage lineages. The CNN was trained in a supervised manner to segment classify and then quantify the lineages across entire tissue sections.

RESULTS: The AI model accurately detected and classified major BM cell populations, demonstrating strong agreement with pathologist assessments of lineage predominance and M:E ratios.

CONCLUSION: This AI model demonstrates the feasibility and utility of automated, quantitative BM evaluation in rat toxicology studies.

IMPACT STATEMENT: Integration of AI-assisted BM lineage enumeration can enhance sensitivity for detecting hematopoietic changes, reduce evaluation time, and improve consistency across studies and observers. Continued refinement and validation may enable broader adoption of AI-based tools to support pathologist decision-making in nonclinical safety assessment.

P47 Performance of a Single-Class Unsupervised Foundation Model-Based AI Histology Anomaly Detector on Rat Heart from Nonclinical Toxicology Studies

Thomas Forest[1], Tiffany Jenkins[1], Roujia Wang[1], Kyathanahalli Janardhan[1], Takayuki Tsuchiya[1], Rajath Soans[1], Lin Li[1], Tosha Shah[1], Raghav Amaravadi[2], Geetank Raipuria[2], Nitin Singhal[2]

[1]Merck & Co., Inc., Rahway, NJ, USA. [2]AIRA Matrix, Mumbai, Maharashtra, India

Abstract

INTRODUCTION: A single-class, unsupervised foundation model-based anomaly detector trained using whole slide images (WSI) of Wistar Han rat hearts from vehicle control groups was studied to understand its utility and limitations for prioritizing histology evaluations in exploratory toxicology studies.

METHODS: Studies conducted in 3 test facilities were selected including 5 treated groups with test article-related cardiac histopathology and 9 treated groups without identified test article-related findings. WSI were analyzed for anomalies. Data collected were annotations highlighting anomalous histology and out of distribution (OOD) score (affected tissue area/total tissue area). Annotations and OOD-scores were compared with pathologist diagnoses.

RESULTS; Annotations accurately highlighted regions of cardiac histology different from vehicle controls. OOD-scores from a study conducted in 1 of the 3 test facilities were not comparable to other studies due to an increase in anomaly detections in the auricles attributable to a histology artifact in the specimens. Using a threshold based on concurrent controls, OOD-scores were insensitive for flagging WSI for review that containing small foci of myocardial degeneration, although the degenerative foci were correctly annotated as different from control. In one treated group, OOD-scores and annotations flagged a cardiac histomorphology finding attributable to test article not considered noteworthy by the pathologist.

CONCLUSION: Single class unsupervised anomaly detection shows promise as a screening tool for heart histology slides from nonclinical studies, however, utility depends on tight control of preanalytical variables. Moreover, simple summation metrics, such as OOD-score can be insensitive to focal histopathology findings.

P48 Enumeration and Laser Capture of Lung Cancer Metastasis in a Mouse Model Using AI Workflows

Raisa Glabman, Amanda Koehne, Jacob Kennedy, Shivani Srivastava

Fred Hutch Cancer Center, Seattle, WA, USA

Abstract

BACKGROUND: Recent advances in artificial intelligence (AI) have the potential to transform cancer research by enhancing imaging, digital pathology, genomics, and data analysis. Currently, the task of quantifying tumor metastases in the lungs of experimental mice relies on manual counting, a process that is time-consuming, prone to intra-observer variability, and challenging to interpret. Additionally, downstream applications such as laser capture microdissection (LCM) require redundant manual annotations and labor-intensive tasks.

METHODS: 58 H&E stained whole slide images (WSI) were used to develop an AI-based classifier to detect lung metastases in a genetically engineered mouse (GEM) model of human non-small cell lung cancer (NSCLC). AI (Aivia AI) was also integrated into workflows for image analysis and LCM to streamline spatial proteomic analysis.

RESULTS: Utilizing an AI-based classifier to detect lung metastases improved sensitivity, accuracy, and quantitative outputs such as tumor area and percentage. Replacing manual dissection with automated tools optimized efficiency and increased precision and reproducibility in the LCM and proteomic workflow.

CONCLUSION: The integration of AI enhanced both accuracy—by reducing error and bias through pathologist-informed training—as well as efficiency and throughput—by automating repetitive tasks, facilitating remote access, and improving quality control.

IMPACT: The resulting algorithms are adaptable, allowing future users to refine them using their own data and images.

P49 Automated Quantification of Airway Epithelial Cell Composition in Complex *In Vitro* Models Using Deep Learning–Based Image Analysis

Van Hovenga[1,2], Steven Laing[2], Christy Chu[2], Daniel Simmons[2], Mike Reichelt[2], Lenitza Nives Lopez[2]

[1]University of California, Berkeley, CA, USA. [2]Genentech, South San Francisco, CA, USA

Abstract

INTRODUCTION/OBJECTIVES: Complex *in vitro* airway models (CIVMs), including lung-on-chip (LOC) and transwell systems, are new approach methodologies (NAMs) to assess airway pharmacodynamic and toxicity responses. However, scalable, objective quantification of epithelial cell composition remains limited. We developed an automated pipeline to quantify basal, ciliated, and secretory cells and characterize differentiation dynamics.

EXPERIMENTAL DESIGN/METHODS: Wide-field ultrastructure backscattered scanning electron microscopy (BSEM) images (n ≈ 800) from 44 CIVM samples were analyzed. Fourteen annotated images from seven slides were used for training/validation. Our pipeline combined U-Net-based tissue segmentation with YOLO-based cell detection. Performance was evaluated via k-fold cross-validation.

RESULTS: Segmentation performance was high (Dice ≈0.96; IoU ≈0.92). Detection showed relative absolute cell count error of 0.20 (basal), 0.20 (ciliated), 0.12 (secretory), and 0.17 overall, with no LOC-transwell bias. Secretory cells were most reliably detected; basal and ciliated cells were undercounted. Pre-air-liquid interface (ALI) to 6 weeks post-ALI, LOC models showed decreasing basal cells, transiently increasing then declining ciliated cells, and increasing secretory cells, yielding a rise then fall in the ciliated:secretory ratio. Transwells showed stable basal cells, gradual ciliated increases, and persistently elevated secretory cells, with minimal ratio change.

CONCLUSION: Deep learning-based quantification of BSEM images allows for tracking of airway differentiation trajectories and complements RNA-based assessments. However, the small training set limits generalizability and a larger dataset would improve model performance.

IMPACT STATEMENT: This approach enables high-throughput, quantitative evaluation of airway model fidelity and cell-type-specific responses, advancing toxicologic assessment and NAM adoption.

P50 Optimization of *In Situ* Hybridization (ISH) Staining in Human Tissue Microarrays: Addressing RNA Quality and Background in Challenging Tissues

Emily M. King, Kevin Maisonave, Lydia Andrew-Jones, Amanda Krempley, Magali Guffroy, Stacey Fossey

AbbVie, North Chicago, IL, USA

Abstract

Tissue microarrays (TMAs) enable rapid, cost-effective screening of multiple tissue types from numerous donors within a single experiment, offering unique advantages for high-throughput RNA detection and biomarker studies. Currently, no standardized or optimized protocols exist for *in situ* hybridization (ISH) analysis specific to TMAs, despite growing use in research. This study focuses on optimization using a peptidylprolyl isomerase B (PPIB) probe. PPIB serves as an effective positive control due to its ubiquitous expression in cells, enabling a comprehensive assessment of RNA preservation quality across the multiple tissues and donors in a typical TMA. Tissue preservation quality can vary in human TMAs, which may be sufficient for immunohistochemistry but not ISH. TMA vendor selection utilizing RNA integrity assessments can improve optimization of the strength and consistency of PPIB ISH signal in most tissues. Once quality of RNA preservation is ascertained, use of the PPIB probe enables optimization of variables such as tissue fixation, epitope retrieval, and protease treatment for a given TMA.

Specific tissues (i.e. esophagus, pancreas and renal tubules) have intrinsic properties such as endogenous peroxidase activity that can lead to heightened background staining. Achieving robust signal-to-noise in problematic tissues requires tailored strategies, including enhanced RNase-free handling, whole-tissue analysis, and possible additional amplification steps. These optimizations increase reproducibility of quantitative and qualitative RNA mapping in TMAs, establishing a foundation for the development of consistent tissue-based biomarker or expression assessment. Our work provides an adaptable workflow for ISH assay development, addressing common pitfalls encountered with background staining and variable quality.

P51 Uncharted Territories: Leveraging MALDI-MSI in the Canine Brain as a Novel Translational Neurology Platform

Sophie R. Nelissen[1], *Rinat Abzalimov*[2], *Shu Zhang*[2], *Elena A. Demeter*[1]

[1]Cornell University College of Veterinary Medicine, Ithaca, NY, USA. [2]CUNY Advanced Science Research Center, New York, NY, USA

Abstract

INTRODUCTION: Canine neurodegenerative (ND) and neuroinflammatory (NI) diseases are considered potential spontaneous models of human neurological disorders. Though pathologically altered cerebral lipidomics correlate with human ND/NI diseases, canine spatial metabolomics remain uncharacterized. Hence, unraveling canine cerebral lipidomics represents an untapped translational avenue.

EXPERIMENTAL DESIGN: MALDI-MSI analysis was conducted on 2 canine brain sections collected within 2 hours of euthanasia. Tissue was either formalin-fixed, paraffin-embedded (FFPE), or embedded in 4% carboxymethylcellulose and frozen. Analysis focused on major structural lipids: glycerophospholipids, ceramides, sphingomyelin, gangliosides, and cardiolipins. Because FFPE sections must be deparaffinized prior, the lipid analyte yield was compared between FFPE and fresh-frozen sections (FF).

METHODS: Tissue samples were sectioned and mounted on indium tin oxide-coated glass slides. FFPE sections were deparaffinized with xylene and treated with heat/pressure-based antigen retrieval. Slides were sprayed with an NEDC matrix and analyzed with a Bruker timsTOF fleX mass spectrometer in negative mode. Data was analyzed using the SCiLS MALDI Imaging software. Analytes were tentatively annotated on their mass-to-charge ratio (m/z) and collision cross section (CCS) values; one heatmap was generated per target analyte.

RESULTS: Structural lipids had a similar distribution between FFPE and FF brain sections, and mirrored the anatomical distribution recorded in humans.

CONCLUSION: MALDI-MSI reliably maps structural lipids in the healthy canine brain, thereby supporting transposability of the method to diseased canine tissues.

IMPACT STATEMENT: MALDI-MSI-based spatial metabolomics is a completely novel comparative avenue that is bound to uncover underlying cerebral metabolic alterations in canine patients and accelerate cross-species therapeutic target discovery.

P52 Teratoma Formation Assay in Immunocompromised Mice to Evaluate Risk of Pluripotent Stem Cell-Derived Cell Therapy Products

Tyler J. Peat[1], *Sasmita Mishra*[1], *Brian E. McIntosh*[2], *Mayuri S. Prasad*[2], *Susan Lynk*[2], *Pamela E. Blackshear*[1]

[1]Labcorp, Greenfield, IN, USA. [2]Labcorp, Madison, WI, USA

Abstract

INTRODUCTION: Human pluripotent stem cell (hPSC) derived products show promise in regenerative medicine for treating myriad diseases. However, safety concerns exist from residual undifferentiated cells forming teratomas, tumors comprised of tissues from three different germ layers. To assess tumorigenicity risk of hPSC-derived therapies, an *in vivo* teratoma formation assay was developed.

METHODS: NSG mice were administered 50% v:v basement membrane extract: cell culture media (vehicle control, n=2) or 1x106 ACS-1021 (iPSCs line derived from human fibroblasts in vehicle, n=6) via quadriceps muscle injection. Mass measurements were obtained prior to dosing and through the study duration. Mice were humanely euthanized after 84 days, or at 64 or 78 days due to impediment of movement, and masses/quadriceps muscle were fixed in 10% neutral buffered formalin, processed, sectioned and stained with H&E or immunohistochemically for human nucleoli (HuNu) antibody, PAX6, Desmin, and SOX17.

RESULTS: Benign teratomas noted in 4/6 mice administered ACS-1021 iPSCs correlated with masses observed at necropsy. Teratomas were characterized by HuNu+ cells effacing surrounding skeletal muscle comprised of well-differentiated tissues from three germ cells layers as follows: neuron like cells and/or cysts lined by ependymal cells or stratified squamous epithelium (PAX6 positive; ectoderm); bundles of smooth muscle and scattered foci of mature cartilage (Desmin positive; mesoderm); and cysts lined by ciliated, pseudostratified columnar epithelium, and/or ducts and acini lined by cuboidal to columnar epithelial cells (SOX17 positive; endoderm).

CONCLUSION: The ACS-1021 iPSC teratoma assay is a useful positive control in testing stem cell-derived therapy products.

P53 Agentic Artificial Intelligence System for Preclinical Toxicologic Study Report Drafting via Integrated Data Analysis, Research and Reasoning

Nasir Rajpoot, Adnan Khan, Mostafa Jahanifar, David Snead
Histofy Ltd, Coventry, United Kingdom

Abstract

INTRODUCTION/OBJECTIVES: Preclinical toxicologic pathology reporting requires integration of heterogeneous data sources, including histopathology, clinical pathology, study metadata and deep web sources. This process is time-intensive and variable. We present an agentic AI system designed to accelerate and standardise preclinical toxicology workflows through structured data interrogation and evidence synthesis.

METHODS & MATERIALS: The proposed system integrates histopathology annotations, clinical pathology data, and study reports. It uses tool-based reasoning to retrieve and contextualise findings from internal data and external biomedical sources, generating structured, evidence-linked outputs.

EXPERIMENTAL DESIGN: The system was evaluated using representative preclinical toxicology datasets. Performance was assessed by comparing accuracy across query resolution, reasoning, robustness, and validity against a general-purpose AI baseline, alongside estimated reductions in report drafting time.

RESULTS: The proposed system demonstrated high accuracy across all evaluation dimensions: query resolution (95.6%), reasoning (89.3%), robustness (87.5%), and validity (100%), with an overall accuracy of 92.8%. This substantially outperformed the general-purpose AI baseline (27.6%, 19.8%, 15.0%, 0%, and 23.1%, respectively). Use of the system resulted in an estimated 60–80% reduction in time required for first-pass study report drafting, with improved consistency and traceability of outputs.

CONCLUSION: An agentic AI approach enables efficient integration of complex study data and supports rapid, structured, evidence-based reporting in toxicologic studies.

IMPACT STATEMENT: This work introduces a workflow-level AI paradigm for preclinical toxicology, enabling scalable, standardised reporting with improved efficiency, consistency, and traceability in preclinical drug development.

P54 A Cell-Based Protein Array, the Membrane Proteome Array (MPA), to Assess Off Target Binding Across the Full Human Membrane Proteome

Jonathan Richards, Diana Norden, Carmen Navia, J. Tabb Sullivan, Benjamin J. Doranz
Integral Molecular, Philadelphia, PA, USA

Abstract

Investigational new drug (IND) applications for biotherapeutics require detailed specificity analysis for safety profiling to uncover potential off-target effects. Tissue cross-reactivity (TCR) studies have conventionally been employed to screen for off-target binding; however, their predictive value regarding *in vivo* safety and toxicity is limited. To address this challenge, we developed a cell-based protein array, the Membrane Proteome Array (MPA), to assess binding across the full human membrane proteome. The MPA encompasses ~6,000 membrane proteins, each individually expressed in their native structural configuration within unfixed human cells. The MPA assesses binding interactions by high-throughput flow cytometry, allowing for high sensitivity detection and quantitative analysis. Here, we used the MPA to estimate the frequency of off-target binding by candidate antibody therapeutics. A retrospective analysis of 250 customer preclinical antibodies screened using the MPA indicated a surprisingly high off-target rate, with 33% of lead candidates displaying off-target binding. Moreover, about 20% of therapeutic antibodies in clinical development and currently on the market displayed off-target binding. To directly compare cell-based protein arrays to TCR studies, we compared our own MPA data to publicly available TCR data and in several cases identified discrepancies in off-target binding results. Overall, the presented case studies and off-target rates at the different phases of drug approval suggest that off-target binding is a major cause of adverse events and drug attrition that could be ameliorated with better specificity screening. The MPA is currently being qualified as a novel Drug Development Tool through FDA's ISTAND program.

P55 Unsupervised Deep Learning-Based Image Analysis Model for Detecting Unlearned Findings in Rat Testis

Taishi Shimazaki[1], Yuzo Yasui[1], Naohito Yamada[1], Vedang Kshirsagar[2], Saketh Juturu[2], Pranab Samanta[2], Raghav Amaravadi[2], Toshiyuki Shoda[1]

[1]Shionogi & Co., Ltd., Yokohama, Kanagawa, Japan. [2]AIRA Matrix, Thane, Maharashtra, India

Abstract

INTRODUCTION: We previously developed supervised models capable of accurately detecting known abnormalities in Whole Slide Images (WSIs) of the liver, kidney, testis, epididymis and brain. However, the models developed based on supervised approaches were unable to identify unlearned findings with sufficient accuracy. We developed a model using unsupervised development approaches into the current image analysis framework for rat testis and assessed its performance in identifying various toxicity findings.

MATERIALS AND METHODS: Vehicle control testis 100 WSIs from 8- to 10-week-old male Sprague-Dawley rats were utilized to build an unsupervised learning model. The WSIs showing both learnt or unlearned features were analyzed, and the results were compared with histopathological diagnoses provided by JSTP-certified pathologists.

RESULTS: The model to identify testicular findings, including unlearned findings, was superior to that of the previous supervised learning models. Additionally, the accuracy was generally consistent with the histopathological diagnosis made by the pathologists. Moreover, the findings overlooked by the previous supervised model could be identified with greater precision.

CONCLUSION: The model was considered highly beneficial as a supplementary tool to histological assessment by pathologists, primarily for screening testicular toxicity in non-GLP early toxicity investigations.

P56 Development of a Predictive Model Combining HPV DNA Genotyping and E6/E7 mRNA Testing for the Diagnosis of Cervical Precancerous Lesions

Jingzheng Ye

Liangping District People's Hospital, Chongqing, China

Abstract

OBJECTIVE: This study aimed to analyze the risk factors for cervical precancerous lesions using a combined approach of HPV DNA genotyping and E6/E7 mRNA testing, and to develop a diagnostic predictive model.

METHODS: A cross-sectional study was conducted among patients with suspected cervical cancer who were admitted to Liangping District People's Hospital and Nanchuan District People's Hospital in Chongqing, China, from February 2023 to July 2025. All participants underwent histopathological examination. The patients with CIN2+ were assigned to the study group(n=86), and others were assigned to control group(n=156).

RESULTS: A total of 242 female patients were included in this study, with a mean age of 42.6±8.9years. Histopathologic findings showed that 27.3%(66/242) patients had inflammation, 37.2%(90/242) had CIN1, 19.0%(46/242) had CIN2, 11.6%(28/242) had CIN3, and 5.0%(12/242) had cervical cancer. The prevalence of HPV16 infection was significantly higher in study group than in the control group [41.9%(36/86) vs 12.2%(19/156), P<0.05]. The study group had a significantly higher E6/E7 mRNA positivity rate compared with the control group [74.4%(64/86) vs 25.0%(39/156), P<0.05]. Multivariable logistic regression analysis showed that HPV16 infection [aOR=3.28(95%CI,1.76–6.10), P=0.01] and E6/E7 mRNA positivity [aOR=5.74(95%CI,3.06–10.77), P=0.01] were risk factors for the development of cervical precancerous lesions. The combined predictive model demonstrated good diagnostic performance [AUC=0.78(95%CI,0.72–0.84)].

CONCLUSION: Both HPV16 infection and E6/E7 mRNA positivity were identified as high-risk factors for the development of cervical precancerous lesions.

P57 Tafazzin Overexpression with High Dose AAV in Tafazzin Knockdown Mice Leads to Cardiotoxicity

Elizabeth L. Buza[1], Nicholas Roberts[1], Christina Chen[1], Swapnil V. Shewale[2], Peter Bell[1], Juliette Hordeaux[1], James M. Wilson[1]

[1]GEMMA Biotherapeutics, Philadelphia, PA, USA. [2]Gene Therapy Program, University of Pennsylvania, Philadelphia, PA, USA

Abstract

Toxicity due to adeno-associated virus (AAV)-induced transgene overexpression following systemic administration has been described in highly transduced cell types such as dorsal root and trigeminal ganglion sensory neurons and liver cells. We investigated the effect of transgene expression levels following systemic administration of heart-targeted AAV vector in a murine model of Barth syndrome (X-linked mitochondrial disease involving cardiomyopathy, skeletal myopathy, biochemical abnormalities, and growth retardation). Tafazzin (TAZ)-knockdown (TAZKD) mice (15-16/group) received a single intravenous injection of heart-targeted AAV vector expressing human TAZ across 4 doses on post-natal day 31. Survival, echocardiography, and serum biomarker (including growth differentiation factor-15/GDF-15, an oxidative stress marker) in-life analyses were conducted; necropsy occurred 110 days post administration. TAZKD mice exhibited elevated GDF-15 and increased left ventricular fractional shortening, but no microscopic findings were detected in the heart. TAZKD mice that received the highest dose (1.0x1014 genome copies/kg) exhibited early morbidity/mortality (9/16 mice) from Day 15-62 due to cardiotoxicity that corresponded with high transgene expression (Western blot, *in situ* hybridization). TAZ overexpression in the hearts of these mice coincided with dilated cardiomyopathy comprising cardiomegaly with biventricular dilatation, cardiomyocyte degeneration and necrosis, fibrosis, and atrial thrombosis in conjunction with higher serum GDF-15 elevations, reduced systolic function (echocardiography), and increased heart-to-bodyweight ratios at necropsy. The dilated cardiomyopathy in TAZKD mice that received the highest AAV dose was considered test article related. Understanding the relationship between dosage, transgene expression, and toxicity is crucial for identifying therapeutic windows during clinical development, particularly for high systemic AAV doses and cardiac applications.

P58 Histologic Method for Nonhuman Primate Tooth Evaluation on Toxicity Studies

Sarah Coe[1], Rachel Stoops[2], Chris Bollinger[2], Deanna Buford[2], Matthew Zipprich[2], Susan Kent[3], Judit Markovits[2]

[1]Inotiv, Kalamazoo, MI, USA. [2]Inotiv, St. Louis, MO, USA. [3]Inotiv, Evansville, IN, USA

Abstract

Evaluation of nonhuman primate (NHP) teeth is rarely performed in toxicity studies, though may be desired to determine whether test article-related dental lesions observed in rodents are relevant to primates/humans. This study aimed to develop a practical method to process NHP teeth in a high-throughput laboratory for toxicity studies.

Two sectioning methods were evaluated in formalin fixed skulls from 2 juvenile Cynomolgus macaques. Method 1 generated sections sagittal to incisors 101 and 401 and the most caudal upper and lower molar (109 and 409). Method 2 adapted standard nasal cavity sections to generate maxillary molar sections, and the incisor and mandibular sections were generated as in Method 1. The samples were decalcified in 7% hydrochloric acid for up to 8 days with two solution changes. The samples were processed and stained routinely with hematoxylin and eosin.

Method 1 produced sections of incisor and molar where dentin, pulp cavity, and tooth root were present in a single plane. Method 1 also captured developing molar teeth, which may prove useful in evaluation of test article-related effects. Method 2 resulted in inconsistent sections of maxillary molar, where major structures were not present in a single plane. If microscopic evaluation of NHP teeth is required for a toxicity study, unilateral sagittal sections of an upper and lower incisor and of the most caudal molar present provide practical, high-quality sections for evaluation. This method provides enhanced evaluation of oral pathology in NHPs and should be utilized in studies where dental toxicity is suspected.

P59 Refreshed ICR Mouse Colony to Eliminate Retinal Degeneration Associated with pde6b Mutation

Sarah Coe[1], Jaymie Voorhees[2], Charlotte Hollinger[1], Sheri Church[3]

[1]Inotiv, Kalamazoo, MI, USA. [2]Inotiv, St. Louis, MO, USA. [3]Inotiv, Indianapolis, IN, USA

Abstract

Moderate retinal degeneration was identified in up to 80% of male and female Hsd:ICR CD-1 mice housed at Envigo vivariums in the USA. A mutation in the pde6b gene (pde6brd1) was identified in the affected colonies, and thus, the Hsd:ICR CD-1 mouse was refreshed using an unaffected ICR colony from the Envigo Netherlands location. The purpose of this study was to confirm retinal health in the refreshed colony.

Mice were divided into two groups. Group 1 was comprised of 5 male and 5 female CD-1 mice from the discontinued colonies. Group 2 was comprised of 10 male and 10 female CD-1 mice from the refreshed colony. Animals were humanely euthanized at approximately 18 weeks of age. Ear punches were collected for genotyping, and ocular tissues were routinely processed for histopathology.

In Group 1, 8/10 mice were homozygous mutant, 1 female was heterozygous, and 1 male was wild type for pde6b-3. In Group 2, 19/20 mice were wild type, and 1 female was heterozygous mutant.

Bilateral, diffuse, moderate outer retinal atrophy occurred in 4/5 homozygous mutant animals from each sex in Group 1. There were no microscopic lesions in the eyes of Group 2 animals in either sex. All optic nerves were microscopically normal in both groups.

In conclusion, retinal degeneration is absent in the refreshed Hsd:ICR CD-1 colony. This colony provides enhanced model quality of Envigo CD-1 mice, which allows for greater nuance in interpretation of ocular findings in toxicity studies.

P60 Comparative Short-Term (5-day) *In Vivo* Repeat Dose Biological Potency Studies of Five *Ginkgo biloba* Extract Lots in Male F344/NCrl Rats: Selected Apical, Clinical Pathology and Toxicogenomic Results

Michelle C. Cora, Cynthia V. Rider, Frederick Parham, Suramaya Waidyanatha, Georgia K. Roberts, Kelly A. Shipkowski, Scott S. Auerbach

Division of Translational Toxicology, National Institute of Environmental Health Sciences, National Institutes of Health, Research Triangle Park, NC, USA

Abstract

INTRODUCTION: Botanical extracts are compositionally complex and can vary substantially between lots, complicating interpretation of toxicity data and decisions about whether one mixture is "sufficiently similar" to a reference. To inform sufficient-similarity decisions for *Ginkgo biloba* extract (GBE), short-term (5-day), repeat-dose gavage studies in male F344/NCrl rats were performed to compare five GBE lots (Lots 1-5); Lot 1 was previously tested in an NTP 2-year study.

EXPERIMENTAL DESIGN: Rats were dosed by gavage (0–1000 mg/kg GBE) for 5 days and evaluated for clinical chemistry, hematology, body and organ weights, and gene expression.

METHODS: Dose–response relationships for apical and transcriptomic endpoints were modeled using BMDExpress. Relative potency was calculated as the fold-shift in benchmark-dose (BMD) relative to reference Lot 1. Qualitative similarity was assessed using Pearson correlation and clustering used to evaluate concordance relative to Lot 1. Relative potency and similarity metrics were then integrated across modalities to generate an overall ranking.

RESULTS: Lot 5 showed the greatest overall concordance with Lot 1 across chemistry, clinical pathology, liver weight, CAR/PXR signature, and transcriptomics; Lot 3 showed intermediate similarity and Lots 2 and 4 showed minimal concordance. Bile acids, ALP, cholesterol and A/G ratio were similarly changed in Lots 1, 3 and 5.

CONCLUSION: Integrating chemical, apical, clinical pathology, and transcriptomic BMD metrics provides a robust, mechanism-informed basis for assessing biological similarity among complex mixtures.

IMPACT STATEMENT: These results illustrate how multimodal, dose-responsive approaches can strengthen confidence in mixture similarity determinations and inform decisions about test-article selection and data extrapolation.

P61 Spontaneous Cardiomyopathy in Mauritian-Source Compared to Asian-Source Cynomolgus Macaques: Incidence and Characterization.

Joshua H. Decker[1], Lydia L. Andrews-Jones[1], Wayne R. Buck[1], Stacey L. Fossey[1], Shima Mehrvar[1], Michele R. Phillips[1], Tatiana A. Sharapova[1], David Rehagen[2], Kevin O. Maisonave[1], Edyta Jarmulkowicz[1], Magali R. Guffroy[1]

[1]AbbVie Inc., North Chicago, IL, USA. [2]Charles River Laboratories, Mattawan, MI, USA

Abstract

Cardiomyopathy is a common finding in control cynomolgus monkeys on toxicology studies and is characterized by cardiomyocyte disarray, karyomegaly, interstitial fibrosis, and vacuolation. Mauritian-source monkeys are more prone to this finding than are Asian-source monkeys. Although the pathogenesis is unclear, stress-induced catecholamine release likely has a role.

A retrospective analysis of hearts from 110 Asian monkeys (58 male, 52 female) and 84 Mauritian monkeys (42 male, 42 female) was performed using whole slide images of H&E-stained sections. All monkeys were vehicle control animals with ages ranging from two to 13 years.

Findings consistent with spontaneous cardiomyopathy were present in 7/58 Asian males (12%), 1/52 Asian females (2%), 18/42 Mauritian males (43%), and 21/42 Mauritian females (50%). The incidence and severity of the findings were greater in Mauritian monkeys and were greater in animals aged ≥4 years than in animals aged ≤3 years. Future work includes additional characterization using special histochemical and immunohistochemical stains, electron microscopy, and genomic and transcriptomic analysis (e.g., RNA sequencing) to compare affected and unaffected animals.

Spontaneous cardiomyopathy in cynomolgus monkeys may confound evaluation of a potential test article-related effect in the heart. When considering whether a given finding may be treatment-related, the entire weight of evidence should be evaluated against the frequent background incidence of spontaneous cardiomyopathy that can be of marked severity in control monkeys, especially in older Mauritian monkeys. Use of Mauritian monkeys in studies of compounds with potential for cardiac liabilities should be carefully considered in study planning.

P62 Feline Valvular and Mural Eosinophilic and Granulomatous Endomyocarditis (Feline Hypereosinophilic Syndrome) with Congestive Heart Failure

Paulina Gomez[1], Jessica Ward[1], Elizabeth Mason[1], Olufemi Fasina[2]

[1]Department of Veterinary Clinical Sciences, Iowa State University, Ames, IA, USA. [2]Department of Veterinary Pathology, College of Veterinary Medicine, Iowa State University, Ames, IA, USA

Abstract

Hypereosinophilic syndrome is a rare systemic disorder in cats characterized by sustained eosinophilia and eosinophil-mediated toxicologic injury and pathology. A 3-year-old castrated male domestic shorthair cat was presented for an acute onset of dyspnea and was diagnosed with left-sided congestive heart failure. Echocardiography revealed concentric left ventricular hypertrophy with hyperechoic and irregular endomyocardium, large, irregular, oscillating lesions involving the mitral valve apparatus, and severe left atrial dilation. Complete blood count revealed a marked leukocytosis (53.33 x103/uL; reference range 5.5-19.5 x103/uL) and marked eosinophilia (11.20 x103/uL; reference range 0.0-0.75 x103/uL). Despite initial stabilization and medical management for congestive heart failure, the cat died due to cardiopulmonary arrest. Gross pathology revealed that the right and left atria were moderately dilated, and the left ventricular chamber was filled with a large tan-to-red clot obstructing the aortic outflow. The mitral valve was thickened and covered by red-to-tan, irregular, and vegetative thrombi. Histopathology examination indicated chronic eosinophilic and granulomatous mitral valvular and mural endomyocarditis with thrombosis and myocardial necrosis. There was multicentric eosinophilic inflammation in the colon, cecum, and mesenteric lymph nodes. This case highlights a unique feline eosinophilic-mediated cardiac pathology associated with hypereosinophilic syndrome as a rare cause of cardiac disease in domestic cats. This is a natural disease that may provide insights into eosinophil-mediated cardiac toxicologic pathology.

P63 Spontaneous Cardiac Findings in Research Colony Cynomolgus and Rhesus Macaques: A 3-Year Survey

Jiashi Feng[1], *Sarah Coe*[2], *Nicholas Vetter*[2]

[1]University of Wisconsin-Madison School of Veterinary Medicine, Madison, WI, USA. [2]Inotiv, Kalamazoo, MI, USA

Abstract

INTRODUCTION: Spontaneous cardiac microscopic lesions are common findings in laboratory macaques. This survey characterizes histologic findings, prevalence, sex and age distribution, and species differences in cardiac lesions of macaques at a Southern US-based contract research organization breeding colony from 2023 to 2025.

MATERIAL AND METHODS: A retrospective review of cases submitted for diagnostic histopathology (2023–2025) was conducted to identify and describe spontaneous cardiac findings in 456 rhesus (*Macaca mulatta*) age 1 month to 26 years old, and 357 cynomolgus macaques (*Macaca fascicularis*) age 2 to 11 years old.

RESULTS: Cardiac microscopic findings were described in 142/813 (17.5%) cases (89/456 rhesus, 53/357 cynomolgus). The most common findings were inflammatory infiltrates, myocarditis, myofiber degeneration, and features of chronic cardiomyopathy including fibrosis and karyomegaly/anisokaryosis. Inflammatory infiltrates, myocarditis, and degeneration occurred more commonly among juveniles and younger adults in cynomolgus monkeys but were more frequent in older adults among rhesus monkeys. Features of cardiomyopathy were more common in rhesus monkeys, with higher incidence in older adults. Primary cardiac causes of mortality/moribundity occurred in 25 animals (17 rhesus, 8 cynomolgus), with myocarditis (12/27) and cardiomyopathy (12/27) being the most common. Trypanosoma infection was confirmed in 7/11 myocarditis mortalities.

CONCLUSION/DISCUSSION: Spontaneous cardiac microscopic findings are relatively common and may be primary causes of moribundity/death among research colony macaques. Understanding the context and normal incidence of these findings is a critical component in research animal care and use.

P64 Procedural-Related Microscopic Observations in Rats with Indwelling Intravenous Catheters in Nonclinical Toxicology Studies

Sarai Milliron[1], *Sherry Morgan*[2]

[1]Frontage Laboratories, Inc., Chicago, IL, USA. [2]Frontage Laboratories, Inc., Concord, OH, USA

Abstract

Intravenous (IV) administration is one of several routes of administration utilized for toxicology studies. In rodents, sites of IV administration include the tail vein, jugular vein, and femoral vein, with a surgical procedure required for catheter and port placement for jugular and femoral vein access. A wide range of microscopic observations are expected in rats with catheterized jugular and/or femoral veins, primarily involving the catheter insertion site (subcutaneous "tunnel"), catheterized veins, heart, and lungs. Presented herein are common and not-so-common microscopic observations in catheterized/ported rats. Common microscopic observations include residual suture material with chronic inflammation, perivascular and vascular chronic inflammation, endothelial hypertrophy/hyperplasia, intimal thickening/proliferation, and thrombosis (cannulated vessel or heart). Less common and rare microscopic observations include secondary embolism (lungs), valvular endocarditis, and bacteremia (sepsis). In toxicology studies utilizing IV administration, particularly those utilizing a catheter/port system, several complications can limit study success such as compatibility between the test article and catheter or infection at the catheter/port placement site extending into the catheterized vessel. In rats, life threatening procedural-related findings, such as right atrial thrombosis and sepsis, can be observed, however it is assumed that procedural-related mortality should not exceed 5%.

P65 Toxicologic Evaluation of RC-0315, a Mesenchymal Stem Cell-Derived Secretome, Following Repeated Intratracheal Administration in Mice

Michael Timaner[1], Tali Fishman-Jacob[1], Michal Steiner[2], Noam Kronfeld[3], Abraham Nyska[4], Yuval Ramot[5,6]

[1]Remedy Cell Ltd., Haifa, Israel. [2]Preclinical Consultant, Rehovot, Israel. [3]HBI Biotech Sciences, Ness Ziona, Israel. [4]Consultant, Tel Aviv, Israel. [5]Faculty of Medicine, Hebrew University of Jerusalem, Jerusalem, Israel. [6]Department of Dermatology, Hadassah Medical Center, Jerusalem, Israel

Abstract

INTRODUCTION: RC-0315 is a chemotherapy-exposed mesenchymal stem cell-derived secretome developed as a potential advanced therapy for idiopathic pulmonary fibrosis (IPF).

OBJECTIVE AND EXPERIMENTAL DESIGN: A GLP-compliant repeated-dose toxicity study was conducted to evaluate the safety of RC-0315 following intratracheal instillation in immunocompetent ICR and immunodeficient SCID mice. Animals received two cycles of three repeated intratracheal instillations of RC-0315 performed within a 7-day period and separated by a two-week interval. Mice were assigned to saline, vehicle, low-dose, or high-dose groups and were monitored for 3 days (main phase) or 13 weeks (recovery phase) post last administration.

RESULTS: No test article-related mortality or toxic clinical signs were observed in either strain. Clinical pathology parameters, body weight, food consumption, and ophthalmologic findings remained within normal limits, with no dose-dependent alterations. Histopathological examination revealed no RC-0315 related adverse findings in the lungs or other organs, and no local toxicity was evident at the site of administration.

IMPACT STATEMENT: These findings support the favorable safety profile of RC-0315 when administered via the clinically intended route. It is noteworthy that the combined use of immunocompetent and immunodeficient mice provided a comprehensive safety assessment and favorable outcome in mice and support the continued clinical development of RC-0315.

P66 Preliminary Studies for Neurotoxicity from Intranasal Exposure of Zinc Oxide Nanoparticles in APOE3 and APOE4 Humanized Mice

Jesse Riker, Shaolin Liu

University of Georgia, Athens, GA, USA

Abstract

INTRODUCTION: Zinc oxide nanoparticles (ZnO NPs) are increasingly utilized in consumer, medical, and industrial products. Several studies have provided evidence for their neurotoxic potential and their ability to cross the blood-brain barrier. Alzheimer's disease and related dementias (ADRD) are also increasing in prevalence with zinc as a proposed environmental risk factor.

METHODS: Scanning electron microscopy was performed on ZnO NPs. The previously published Solution for Nasal and Olfactory Transport (SNOT) (O'Connell et al, 2022) was recreated. Agglomeration under different sonication energies was assessed via static light scattering. SNOT with ZnO NP and dextran dye was delivered intranasally in mice and translocation to the brain was assessed via fluorescent stereomicroscopy. Pre-dosing novel object recognition (NOR) and buried food testing was performed on a genetic susceptibility model of ADRD (APOE3 and APOE4 humanized mice; n = 8 for each genotype and sex group).

RESULTS: The ZnO NPs were 52.97 ± 19.61nm and primarily globoid in shape. A sonication energy of 200J/mL was determined to minimize ZnO NP agglomeration, which showed positive immunofluorescence in the olfactory bulbs following intranasal exposure. Baseline memory and olfaction were not different between APOE genotypes, but males outperformed females in NOR tests.

CONCLUSION: A method of intranasal delivery of ZnO NPs was successfully established and baseline, pre-dosing behavioral data was obtained for APOE3 and APOE4 humanized mice.

IMPACT STATEMENT: These preliminary data establish the groundwork needed for future ZnO NP intranasal nanotoxicity studies in an ADRD genetic susceptibility model. Post-dosing behavioral and histopathologic evaluation are currently being processed.

P67 Retrospective Study of Infectious Cardiac Lesions in Old and New World Nonhuman Primates: Morphologic Spectrum, Etiologies, and Implications for Toxicologic Pathology

Vinay Shivanna, Donna Perry, Edward Dick, Olga Gonzalez

Southwest National Primate Research Center at the Texas Biomedical Research Institute, San Antonio, TX, USA

Abstract

INTRODUCTION: This retrospective study evaluated cardiac lesions in a research colony of Old-World and New-World nonhuman primates (NHPs).

EXPERIMENTAL DESIGN: Necropsy datasets since 1980 were retrospectively queried for non-experimental inflammatory cardiac lesions across various NHP species.

RESULTS: Cardiac lesions with infectious etiology comprised ~2.5% of all non-experimental morphologic findings. The spectrum of lesions was broad and predominantly inflammatory, with myocarditis being most common, followed by hydropericardium, pericarditis, epicarditis, and endocarditis. Myocarditis was identified across multiple NHP species, including baboons, rhesus, and cynos. The predominant etiologic agent was *Trypanosoma cruzi*, characterized by lymphoplasmacytic inflammation, myocardial degeneration and necrosis, fibrosis, and occasional protozoal cysts. Additional etiologies included encephalomyocarditis virus (*Cardiovirus rueckerti*) (EMCV), *Streptococcus pneumoniae,* and *Staphylococcus aureus*, Hydropericardium was observed in baboons, rhesus, and cynos, and was frequently associated with EMCV, *S. pneumoniae,* and *T. cruzi*. Pericarditis was primarily documented in baboons and cynos, with similar causes- EMCV, *S. aureus, S. pneumoniae,* and *T. cruzi*. Endocarditis was infrequent across species but seen in cynos, rhesus, and baboons. *Staphylococcus aureus* was confirmed in at least one case. Epicarditis was noted across a wider species, including cynos, rhesus, baboons, and marmosets, and was associated in select cases with EMCV, *T. cruzi,* and *S. aureus*.

CONCLUSION: These findings highlight the morphologic heterogeneity and etiologic diversity in NHPs, with implications for differential diagnosis.

IMPACT STATEMENT: This study establishes a morphologic and etiologic framework for interpreting infectious cardiac lesions in preclinical models. By defining the spectrum, frequency, and species distribution of inflammatory cardiac pathology, it supports informed differentiation between spontaneous and test article–related findings and strengthens interpretive rigor.

P68 Chronic Arteriovenous Fistula/Shunt in the Pelvic Limb of a Naïve Peripubertal Cynomolgus Monkey (*Macaca fascicularis*)

Vanessa Vrolyk, Laura Neagu-Lund, Marie-Josée Desmarais

Charles River Laboratories, Laval, Quebec, Canada

Abstract

A naïve 3-year-old peripubertal male Cambodian cynomolgus monkey developed progressive intermittent swelling of the left pelvic limb over two months, beginning shortly after femoral blood collections were performed in the same limb. The swelling was associated with tortuous cutaneous vessels and scab formation. After multiple nonsurgical treatments without improvement, the animal was subsequently euthanized due to clinical deterioration. Gross examination revealed a tortuous vascular network within the subcutis and muscle fascia, with subcutaneous edema, hemorrhages, and enlarged draining lymph nodes. Histologically, diffuse abnormal vascular proliferation extended from above the knee to the foot, involving the dermis, subcutis, skeletal muscle fascia, and epineurium surrounding nerves. Vessels were variably sized, tortuous, occasionally surrounded by myxomatous matrix, microhemorrhages, or mononuclear infiltrates with rare eosinophils, and formed clusters of small vessels in the dermis. Immunohistochemistry showed CD31-positive endothelium and variably thick SMA-positive tunica media, consistent with abnormal arteriolar and venular structures. Numerous Ki67-positive endothelial and smooth muscle cells indicated ongoing proliferation. The findings were most consistent with iatrogenic arteriovenous fistula/shunt originating from the initial venipuncture procedures. Although similar iatrogenic findings have been reported in humans and infrequently in macaques following repeated venipunctures, they are typically localized and reports lack detailed histopathology. This case highlights the histopathologic features of a regionally extensive chronic iatrogenic vascular proliferation and underscore the importance of considering venipuncture history when interpreting vascular findings in the limbs of monkeys used in toxicology studies, particularly when such changes occur in limbs used for intravenous dosing.

P69 Distinguishing Disease-Associated from Test Article-Related Thrombocytopenia in a SHIV-Infected Rhesus Macaque Following AAV-Delivered HIV-1 IgG Therapy

Rachael Wolters[1], *Altair Fazio*[1], *Philip Barnette*[1], *Tracy Ordonez*[1], *Monica Shroyer*[1], *Ann Hessell*[1], *Nancy Haigwood*[1], *Mauricio Martins*[2]

[1]Oregon National Primate Research Center, Beaverton, OR, USA.
[2]The Herbert Wertheim UF Scripps Institute for Biomedical Innovation & Technology, Jupiter, FL, USA

Abstract

Simian–human immunodeficiency virus (SHIV) infection in non-human primates (NHPs) is a model for studying monoclonal antibodies (mAbs) against HIV. Thrombocytopenia is a complication of SHIV and HIV infection, but also occurs secondary to investigational biologics, including anti-drug antibodies (ADA). Distinguishing test article–related toxicity from disease-associated hematologic changes is critical. This study applied a structured causality assessment to evaluate delayed-onset thrombocytopenia.

An infant rhesus macaque received a single intramuscular AAV administration encoding anti-SHIV mabs and was monitored >70 weeks. Viral rebound occurred at week 58, and binding ADA was detected at week 60. Platelet counts and antibody levels were measured serially. ART and prednisone were initiated.

The animal maintained viral suppression for >56 weeks post-AAV. Thrombocytopenia confirmed at week 62 (29–74 $\times 10^3$/μL; nadir 29 $\times 10^3$/μL), without anemia, leukopenia, or clinical illness. ADA developed but did not eliminate therapeutic antibody expression. Viral loads increased to $>10^4$ copies/mL and remained elevated. To rule out the potential of antibody-mediated thrombocytopenia, immunocytochemistry showed no IgG binding to platelets. A bone marrow aspirate was not performed due to the risk of hemorrhage. Other animals, including those with viral rebound, did not develop thrombocytopenia. Platelet counts normalized within two weeks of ART and prednisone initiation.

The lack of anti-platelet antibodies, and response to therapy support thrombocytopenia as a SHIV-associated outcome. HIV induced thrombocytopenia is a life-threatening sequela, this case provides a framework for differentiating potential causes of thrombocytopenia in the context of long-term gene-delivered therapeutic studies in NHPs.

P70 Results of the 2026 Membership-Wide Survey on the Topics of Diversity, Inclusion and Belonging in the Society of Toxicologic Pathology

Agathe Bedard[1], *Christina Alarcón*[2]

[1]Charles River Laboratories, Senneville, Quebec, Canada.
[2]Genentech, South San Francisco, CA, USA

Abstract

INTRODUCTION/OBJECTIVES: The STP Diversity, Inclusion and Belonging (DIB) Committee conducted an inaugural membership-wide climate survey on DIB efforts within the STP in October 2022, which provided key insights into the largely positive member experience as well as identifying areas of potential improvement. The survey was repeated in March 2026 to determine data trends and current progress of the STP DIB efforts. This poster presents the results of the 2026 survey, comparison with data from 2022, and highlights the activities of the STP DIBC.

EXPERIMENTAL DESIGN/METHODS AND MATERIALS: The original 2022 study was designed with 26 questions in consultation with Ascension Worldwide. The 2026 study repeated all the questions from the previous study and included an additional question and free-text section. The survey link was emailed to STP members in Spring 2026. Responses were anonymous and further anonymized by AIM representatives by separating the rubric questions from the free-text responses and removing identifying information (e.g. names, institutional affiliations, etc.) from free-text responses. Anonymized response data was analyzed by authors using a combination of statistical analysis comparable to that used by Ascension Worldwide and AI-supervised analysis.

RESULTS: Pending results from survey (closed March 24, 2026), data will be grouped into: (1.) Participation; (2.) Demographics; (3.) Personal Experience; (4.) DIB Culture; (5.) Other DIBC activities since 2022

CONCLUSION: Pending survey results.

IMPACT: Ongoing efforts in DIBC (including membership-wide surveys) are important to evaluate progress and status of STP DIB community and culture, as well as guide future activities and areas for improvement.